

**T.R.**  
**GEBZE TECHNICAL UNIVERSITY**  
**GRADUATE SCHOOL OF NATURAL AND APPLIED SCIENCES**

**THE EFFECTS OF SIK2 ON HUMAN ADIPOCYTE SECRETOME**  
**UNDER ER STRESS CONDITION**

**NAZLI ERTÜRK**  
**A THESIS SUBMITTED FOR THE DEGREE OF**  
**MASTER OF SCIENCE**  
**DEPARTMENT OF MOLECULAR BIOLOGY AND GENETICS**

**GEBZE**  
**2017**

**T.R.**

**GEBZE TECHNICAL UNIVERSITY**

**GRADUATE SCHOOL OF NATURAL AND APPLIED SCIENCES**

**THE EFFECTS OF SIK2 ON HUMAN ADIPOCYTE  
SECRETOME UNDER ER STRESS CONDITION**

**NAZLI ERTÜRK**

**A THESIS SUBMITTED FOR THE DEGREE OF  
MASTER OF SCIENCE**

**DEPARTMENT OF MOLECULAR BIOLOGY AND GENETICS**

**THESIS SUPERVISOR**

**ASSOC. PROF. DR. FERRUH ÖZCAN**

**GEBZE**

**2017**

**T.C.**  
**GEBZE TEKNİK ÜNİVERSİTESİ**  
**FEN BİLİMLERİ ENSTİTÜSÜ**

**SIK2'NİN ER STRES KOŞULLARI ALTINDA**  
**İNSAN YAĞ HÜCREŞİ SEKRETOMUNA ETKİSİ**

**NAZLI ERTÜRK**  
**YÜKSEK LİSANS TEZİ**  
**MOLEKÜLER BİYOLOJİ VE GENETİK ANABİLİM DALI**

**DANIŞMANI**  
**DOÇ. DR. FERRUH ÖZCAN**

**GEBZE**  
**2017**



## YÜKSEK LİSANS JÜRİ ONAY FORMU

GTÜ Fen Bilimleri Enstitüsü Yönetim Kurulu'nun 18/01/17 tarih ve 2017/04 sayılı kararıyla oluşturulan jüri tarafından 10/02/2017 tarihinde tez savunma sınavı yapılan Nazlı ERTÜRK'ün tez çalışması Moleküler Biyoloji ve Genetik Anabilim Dalında YÜKSEK LİSANS tezi olarak kabul edilmiştir.

### JÜRİ

ÜYE

(TEZ DANIŞMANI) : Doç. Dr. Ferruh ÖZCAN

ÜYE

: Doç. Dr. Nuri ÖZTÜRK

ÜYE

: Doç. Dr. İbrahim YAMAN

### ONAY

Gebze Teknik Üniversitesi Fen Bilimleri Enstitüsü Yönetim Kurulu'nun

...../...../..... tarih ve ...../..... sayılı kararı.

İMZA/MÜHÜR

## SUMMARY

Obesity is a global epidemic and risk factor for metabolic and neurodegenerative diseases, some cancer types related to dysregulation of protein and energy homeostasis. Unresolved ER stress and accompanying inflammatory macrophage accumulation in adipose tissue underlie development of various metabolic dysregulations marked by insulin resistance leading to obesity and T2D. Intriguingly, increased level and activity of SIK2 in murine adipocytes of obese mice is in stark contrast to those detected in obese human subjects. ER stress is triggered when protein synthesis, folding, secretion are failed. The disruption of ER homeostasis induces UPR. Upon chronic ER stress, IRE1 $\alpha$  activates RIDD which directs cells to apoptotic pathways. We reported significant changes in the expression profiles of select adipokines in murine 3T3-L1 cells under ER stress. SIK2 was also reported to favor proinflammatory cytokine production by blocking to CREB-CRTC3 mediated pathway required for M1-M2 switch in macrophages. Based on these data we speculated that altered SIK2 activity and level observed in adipocytes from obese animal models and human subject may be relevant to altered adipokine profiles contributing to pathogenesis of the disease. Earlier findings indicated that SIK2 is required for ERAD and autophagy in response ER stress. We speculated that SIK2 might also contribute to raise of inflammatory response under ER stress conditions by potentiating TRAF-IKK-NF $\kappa$ B axis downstream of IRE1.

In order to get better insight into SIK2 mediated changes in inflammatory outputs we used human preadipocytes LiSa-2 stably expressing either wild type IRE1 $\alpha$  or its RIDD mutant (IRE1<sup>K888A</sup>) along with the SIK2-WT.

**Key Words: ER Stress, SIK2, UPR, IRE1 $\alpha$ , RIDD.**

## ÖZET

Obezite, dünya çapında yaygın bir hastalık olup metabolik ve nörodejeneratif hastalıklar, protein ve enerji dengesindeki düzensizliklerle ilişkili bazı kanser tipleri için büyük bir risk faktörüdür. İnsülin direnciyle başlayan, Tip 2 diyabete ve obeziteye yol açan çeşitli metabolik düzensizliklerin gelişmesinin altında, çözülmemiş ER stresi ve buna eşlik eden yağ dokusundaki inflamatuvar makrofaj birikimi yatar. Merak uyandırıcı şekilde, obez farelerin yağ hücrelerindeki yüksek SIK2 seviyesi ve aktivitesi, obez insanlarda ölçülenlerle büsbütün zıtlık içindedir. Protein sentezi, katlanması ve salgılanması gibi önemli biyolojik mekanizmaların aksaması sonucunda ER stres tetiklenmektedir. ER'deki dengenin bozulması Katlanmamış Protein Cevabının oluşmasına zemin hazırlamaktadır. Kronikleşen ER stresiyle, IRE1 $\alpha$ , İlişkili Yıkım mekanizmasını aktive ederek hücreleri apoptotik yollara yönlendirir. ER stres durumunda fareye ait 3T3-L1 hücrelerindeki seçilmiş adipokin ifade profillerindeki önemli değişiklikleri raporladık. Ayrıca, SIK2'nin M1-M2 makrofaj dönüşümü için gerekli olan CREB-CRTC3 yolağını engelleyerek pro-inflamatuvar sitokin üretimini desteklediği de bildirilmiştir. Bu bilgilere dayanarak, obez insan ve hayvan modellerinin yağ hücrelerindeki değişen SIK2 aktivitesi ve seviyesinin hastalık patojenezine katkı sağlayan değişen adipokin profilleriyle ilişkili olabileceği kanısına vardık. Önceki bulgular ER stresine cevaben SIK2 nin ER ilişkili yıkım mekanizması ve otofaji için gerekli olduğunu göstermiştir. SIK2 nin IRE1'in TRAF- IKK-NF $\kappa$ B ekseninin alt akımını güçlendirerek, ER stress şartları altında, inflamatuvar cevabın ayrıca yükselmesine katkıda bulunabileceğini kanısına vardık.

SIK2 aracılı inflamatuvar sonuçlarındaki değişikliklerin iç yüzünü daha iyi anlamak için stabil olarak yabancı tip IRE1 $\alpha$  veya onun IRE1 $\alpha$  İlişkili Yıkım mutantını (IRE1<sup>K888A</sup>) ifade eden LiSa-2 insan öncül yağ hücreleriyle birlikte yabancı tip SIK2 kullandık.

**Anahtar Kelimeler: ER Stresi, SIK2, UPR, IRE1 $\alpha$ , RIDD.**

## ACKNOWLEDGEMENTS

First of all, I would like to thank my advisor, Assoc. Prof. Ferruh ÖZCAN for his support, encouragement, suggestions and help during whole my study.

I would also thank to my committee members Assoc. Prof. Nuri ÖZTÜRK and Assoc. Prof. İbrahim YAMAN for their criticism.

I would like to thank my precious lab partner İlkey Göksu POLAT for her cooperation, support and of course friendship.

I wish to express my sincere thanks to the members of Obedia Lab; Betsi KÖSE, Mehmet Soner TÜRKÜNER and Özge ÖNLÜTÜRK.

I am also grateful to Furkan ALKAN and Tuğçe KESKİNER for their helps.

I would like to appreciate the helps and friendly environment provided by Axan Lab members, Oya ARI, Başak KANDEMİR, Melis SAVAŞAN SÖĞÜT, Merve ÜSTÜN, Yiğit Koray BABAL, Nil TÜRKÖLMEZ and Eray ŞAHİN.

Finally, I must express my very profound gratitude to my parents Serpil ERCIYAS, Nihat ERCIYAS and to my husband Ceyhun ERTÜRK for providing me with unfailing support and continuous encouragement throughout my years of study and through the process of researching and writing this thesis.

# TABLE OF CONTENTS

	<b><u>Page</u></b>
SUMMARY	v
ÖZET	vi
ACKNOWLEDGEMENTS	vii
TABLE OF CONTENTS	viii
LIST OF ABBREVIATIONS AND ACRONYMS	x
LIST OF FIGURES	xiii
LIST OF TABLES	xiv
1. INTRODUCTION	1
1.1. Aim of the Study	1
2. ADIPOSE TISSUE	2
2.1. Types of Adipose Tissue	2
2.2. Obesity, Insulin Resistance, Type 2 Diabetes	3
2.3. Metabolic Inflammation	5
2.4. Endocrine Function of Adipose Tissue	5
3. ENDOPLASMIC RETICULUM	9
4. ENDOPLASMIC RETIKULUM STRESS	12
5. UNFOLDED PROTEIN RESPONSE (UPR)	14
5.1. PERK Pathway	15
5.2. ATF6 Pathway	16
5.3. IRE1 Pathway	17
5.3.1. IRE1 and Inflammatory Response	19
5.3.2. Regulated-IRE1 $\alpha$ -Dependent Decay (RIDD)	20
6. SALT-INDUCIBLE KINASE FAMILY	26
6.1. SIK2	27
6.1.1. SIK2 and Insulin Sensitivity	27
6.1.2. SIK2 and Inflammatory Response	28
6.1.3. The Relation Between SIK2 and p97/VCP Mediated ERAD	30
7. MATERIALS	31
7.1. Cell Lines and Plasmids	31

7.2. Chemicals	31
7.3. Solutions	32
7.4. Kits	33
7.5. Equipments	34
8. METHODS	35
8.1. Cell Culture and Passaging	35
8.2. Freezing of Cells	35
8.3. Defrosting of Cells	35
8.4. Protein Isolation, BCA, Protein Preparation	36
8.5. SDS-PAGE and Western Blotting	37
8.6. Transformation	38
8.7. Plasmid Isolation	38
8.8. Lentiviral Transfection	39
8.9. Transient Transfection	39
8.10. Site Directed Mutagenesis	40
8.11. RNA Isolation	41
8.12. cDNA Synthesis	42
8.13. Quantitative Real-Time PCR	42
9. RESULTS	44
9.1. Investigation of Mammalian Homologous Residue of yIRE1 R1039	44
9.2. Confirmation of IRE1 <sup>K888A</sup> Mutant Product by Sequencing	45
9.3. Generation of the Stable Cell Lines of GFP, IRE1-WT and IRE1 <sup>K888A</sup> in LiSa-2 Cells	46
9.4. Gene Expression Levels of LiSa-2 GFP and IRE1-WT Stable Cell Lines	47
9.5. Gene Expression Levels of LiSa-2 GFP and IRE1 <sup>K888A</sup> Stable Cell Lines	49
9.6. Comparison of Gene Expression Levels Between LiSa-2 IRE1-WT and IRE1 <sup>K888A</sup> Stable Cell Lines	50
10. DISCUSSION	51
REFERENCES	56
BIOGRAPHY	64
APPENDICES	65

## LIST OF ABBREVIATIONS AND ACRONYMS

<b><u>Abbreviations</u></b>	<b><u>Explanations</u></b>
	<b><u>and Acronyms</u></b>
g	: Gram
kg	: Kilogram
M	: Molarity
ml	: Milliliter
mM	: Millimolar
nM	: Nanomolar
v	: Volume
V	: Volt
μg	: Microgram
μl	: Microliter
μM	: Micromolar
APS	: Ammonium persulfate
ASK1	: Apoptosis Signal-regulating Kinase 1
ATF4	: Activating Transcription Factor 4
ATP	: Adenosine triphosphate
BAT	: Brown Adipose Tissue
BCA	: Bicinchoninic Acid
BiP	: Binding Immunoglobulin Protein
Bp	: basepair
BSA	: Bovine Serum Albumin
bZIP	: Basic Leucine Zipper Domain
CHOP	: C/EBP homologous protein
ChREBP	: Carbohydrate-responsive-element-binding protein
CO <sub>2</sub>	: Carbon dioxide
CRTC2	: CREB regulated transcription coactivator 2
DMEM	: Dulbecco's Modified Eagle Medium
DMEM/F12	: Dulbecco's Modified Eagle Medium/Ham's F12 Medium
DMSO	: Dimethyl Sulfoxide
DNA	: Deoxyribonucleic Acid

EDTA	: Ethylenediaminetetraacetic Acid
eIF2	: Eukaryotic translation initiation factor 2
ER	: Endoplasmic Reticulum
ERAD	: Endoplasmic Reticulum Associated Degradation
FA	: Fatty Acid
GLUT4	: Glucose Transporter 4
FBS	: Fetal Bovine Serum
HEPES	: 4-(2-hydroxyethyl)-1-piperazineethanesulfonic Acid
IKK	: Inhibitor of Kappa B kinase
IL-10	: Interleukin 10
IRE1	: Inositol-requiring enzyme 1
IRE1-WT	: IRE1 Wild Type
IRE1 <sup>K888A</sup>	: IRE1 K888A mutant
IRF3	: Interferon Regulatory Factor 3
IRS1	: Insulin Receptor Substrate 1
JNK	: c-Jun N-terminal Kinase
LKB1	: Liver Kinase B1
MAVS	: Mitochondrial antiviral-signaling protein
MHC	: Major histocompatibility complex
mRNA	: Messenger RNA
NaCl	: Sodium Chloride
NaF	: Sodium Fluoride
Na <sub>3</sub> VO <sub>4</sub>	: Sodium Orthovanadate
NF-κB	: Nuclear Factor-κB
NLS	: Nuclear Localization Signal
PBS	: Phosphate Buffer Saline
PCR	: Polymerase Chain Reaction
Pen/Strep	: Penicillin/Streptomycin
PMSF	: Phenylmethylsulfonyl Fluoride
PKA	: Protein Kinase A
PKC	: Protein kinase C
PERK	: PKR-like ER kinase
PVDF	: Polyvinylidene difluoride
RER	: Rough Endoplasmic Reticulum

RIG-I	: Retinoic Acid-Inducible Gene 1
RNA	: Ribonucleic Acid
Rpm	: Rotations Per Minute
S1P	: Site-1-Protease
S2P	: Site-2-Protease
SDS	: Sodium Dodecyl Sulfate
SDS-PAGE	: SDS Polyacrylamide Gel Electrophoresis
Ser	: Serine
SER	: Smooth Endoplasmic Reticulum
SIK	: Salt Inducible Kinase
SIK2	: Salt Inducible Kinase 2
SIK2-WT	: SIK2 Wild Type
SOCS 3	: Suppressor of cytokine signaling 3
sXBP-1	: spliced X-Box Binding Protein 1
T3	: Triiodothyronine
TBK1	: TANK Binding Kinase 1
TBS	: Tris Buffered Saline
TBST	: Tris Buffered Saline Tween
TEMED	: Tetramethylethylenediamine
THA	: Thapsigargin
Tm	: Melting Temperature
TNF $\alpha$	: Tumor Necrosis Factor alpha
TRAF2	: TNF receptor-associated factor 2
TXNIP	: Thioredoxin-interacting protein
UBA	: Ubiquitin-associated
UPR	: Unfolded Protein Response
WAT	: White Adipose Tissue
WT	: Wild-Type
XBP-1	: X-box Binding Protein-1

## LIST OF FIGURES

<b><u>Figure No:</u></b>	<b><u>Page</u></b>
2.1: Brown and white adipose tissue.	3
3.1: The structure of ER.	9
4.1: Transportation of native proteins to golgi and translocation of unfolded peptides to cytoplasm by ERAD.	13
5.1: The general structure of the sensors in ER.	14
5.2: ER stress signaling pathways.	15
5.3: The formation of UPR signal by ER-stress activated PERK.	16
5.4: The formation of UPR signal by ER-stress activated ATF6.	17
5.5: The structural profile of IRE1.	18
5.6: The formation of UPR signal by ER-stress activated IRE1.	19
5.7: The unfolded protein response (UPR) and inflammation.	20
5.8: The IRE1–RIDD–RIG-I pathway.	22
5.9: IRE1 intersects with inflammatory pathways.	23
5.10: Evolution of the UPR shows conserved functions in immune responses.	24
6.1: The isoforms of Salt-Inducible Kinase.	26
6.2: The regulation of IL-10 production by LKB1-SIK-CRTC3.	29
9.1: The crystal structures of the superimposed forms of yIRE1(blue) and hIRE1(claret red).	44
9.2: The structural change of hIRE1 after the mutation changing Lysine to Alanine.	45
9.3: The p-Lenti-III-HA vector backbone map.	45
9.4: The part of the sequence showing the mutated residue of hIRE1.	46
9.5: Confirmation of IRE1 overexpression with Western Blot.	47
9.6: Gene expression changes of LiSa-2 GFP and IRE1-WT cells upon SIK2-WT transfection and thapsigargin treatment.	48
9.7: Gene expression changes of LiSa-2 GFP and IRE1K888A cells upon SIK2-WT transfection and thapsigargin treatment.	49
9.8: Comparison of gene expression levels between LiSa-2 IRE1-WT and IRE1 <sup>K888A</sup> cells upon SIK2-WT transfection and thapsigargin treatment.	50

## LIST OF TABLES

<b><u>Table No:</u></b>	<b><u>Page</u></b>
7.1: Kits used.	33
7.2: Equipments used.	34
8.1: The solutions used for preparation of gels.	37
8.2: Components for PCR.	40
8.3: Cycling conditions of PCR Program.	40
8.4: Kinase, Ligase and DpnI (KLD) Reaction.	41
8.5: Components for cDNA Synthesis from isolated RNA.	42
8.6: PCR Program for cDNA Synthesis.	42

# 1. INTRODUCTION

## 1.1. Aim of the Study

Obesity, one of the most prevalent problem in the world, is an important risk factor for human health. It is related with several diseases such as diabetes, cardiovascular disease, hypertension and dyslipidemia. In obese animals and human subjects fat expansion is mediated by both increase in adipocyte size (hypertrophy) and number (hyperplasia). However only the former is associated with chronic ER stress and the production of inflammatory cytokines. It is thought that adipose driven proinflammatory cytokines including  $TNF\alpha$ , IL6, IL17, IFN $\gamma$  underlie the development of peripheral insulin resistance pertinent to disease progression. The aim of this study is to evaluate the possible role of SIK2 in shaping the inflammatory response mediated primarily by the RIDD activity of IRE1 in human liposarcoma derived preadipocyte cell line LiSa-2. To achieve this LiSa-2 cells stably expressing IRE1 mutant lacking the XBP1 splicing activity were generated. It is plausible to speculate that depending on the duration and the intensity of ER stress adipocytes with polarized RNase activity towards RIDD would engage either in adipokine secretion or apoptosis. To test this hypothesis we investigated the secretome profiles of human adipocytes stably expressing IRE1 wild type or K888A mutant (selective activation of RIDD) in the presence or absence of SIK2 activity under chemically induced ER stress condition. We hope that our study will improve our understanding of SIK2 mediated changes in ER homeostasis abrogation of which frequently associated with various metabolic and neurodegenerative diseases and some cancers.

## **2. ADIPOSE TISSUE**

Adipose tissue is a complex and metabolically active organ that stores excess energy and also it is considered as a highly active endocrine organ that synthesizes several compounds which control the homeostasis, glucose and lipid metabolism, inflammation. This highly dynamic tissue is composed of adipocytes, endothelial cells, fibroblasts, immune cells such as macrophages and lymphocytes [Ahima and Flier, 2000].

Adipocytes express and secrete various endocrine hormones that are called adipokines. These adipokines are the circulating hormones that are responsible for the communication with other organs containing muscle, brain, liver, immune system and adipose tissue. In the case of the dysregulation of these hormones, metabolism may encounter many diseases such as obesity, type 2 diabetes and cardiovascular disease [Kwon and Pessin, 2013].

### **2.1. Types of Adipose Tissue**

The adipose tissue is classified into two groups; brown adipose tissue (BAT) and white adipose tissue (WAT). The adipocytes in these tissues have different functions and morphology. Brown adipose tissue is observed in newborns but is almost absent in adults and it is responsible for thermogenesis. The adipocytes in the brown adipose tissue are smaller than the adipocytes in white adipose tissue. Different-sized lipid droplets and excessive mitochondria in brown adipose tissue oxidize the fatty acids for the heat production. BAT gets its color from vascularization and the existence of thickly compacted mitochondria. It is also passed over by numerous blood vessels. The heat generated by the mitochondria is dispersed to the different parts of the body by the help of these blood vessels [Fonseca et al., 2007], [Saely et al., 2012].

White adipose tissue has a broader functional capacity than brown fat. It is widely distributed in visceral and the subcutaneous tissue which provides mechanical protection and weakens the effect of the shock. WAT is less vascularized than brown fat and they have few mitochondria so low oxidation rate. WAT is capable of accumulating energy and providing it when it is necessary. Because of being a perfect thermal insulator, it has a significant role to maintain the body temperature [Ibrahim,

2010]. WAT also serves as an endocrine organ by secreting adipokines containing leptin, IL-6, TNF $\alpha$  and adiponectin.

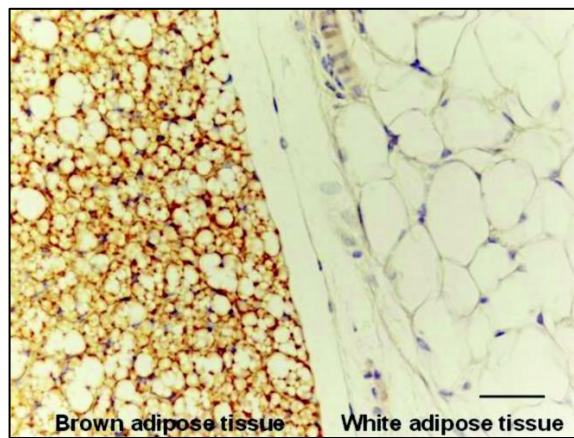


Figure 2.1: Brown and white adipose tissue.

## 2.2. Obesity, Insulin Resistance, Type 2 Diabetes

Excess food intake and sedentary lifestyle enhance enormous accumulation of lipids in adipose tissue which causes obesity. The occurrence of obesity and related diseases is seriously spreading worldwide in both adults and children. In the case of body mass index exceeds 30 kg per m<sup>2</sup>, obesity and its consequent diseases begin to arise [Butler et al., 2003]. When extreme caloric intake and motionless style of living with person's genetic profile are associated, the possibility of obesity is assumed to increase.

Obesity is the major factor which causes the insulin resistance syndrome that contains the type 2 diabetes mellitus, hyperinsulinemia, hyperlipidemia and the possibility of development of the atherosclerotic cardiovascular diseases [Pinhas et al., 1996].

Insulin resistance is a metabolic disorder which prevents cells to respond sufficiently to basal insulin levels and develops initially in muscles, adipose tissue and liver. Under normal conditions, insulin inhibits glucose release from the liver. Onset of insulin resistance make liver to release glucose improperly into the blood.

The development of insulin resistance accelerates subsequent excess fat storage and pro-inflammatory cytokine secretion such as interleukin 6 (IL-6) and tumor necrosis factor  $\alpha$  TNF $\alpha$  by the expanded adipocytes in obesity. Increased secretion of

these factors cause a decrease in the production of adiponectin which is responsible for increasing insulin sensitivity.

When the body shows resistance to the activities of the insulin, pancreas starts to produce increased amount of this hormone which then causes hyperinsulinemia. In this state, the levels of the insulin present in the blood is extremely high when compared with the blood glucose level [Steinberger et al., 1995]. According to the data obtained from different researches display gaining too much weight in childhood and adolescence is related with insulin resistance, high blood pressure and dyslipidemia in early years of adulthood. In the case of losing weight by obese children, insulin concentration begins to decrease and the insulin sensitivity ameliorates [Urbina et al,1999].

T2D is a metabolic syndrome which develops as a result of dysregulated secretion of insulin from pancreatic  $\beta$  cells and showing resistance to insulin of the body especially adipose tissue, liver and muscle. In a healthy individual, the blood glucose levels are regulated with insulin production by  $\beta$ -cells and low blood glucose levels are balanced by the response of liver with production of more glucose. In T2D, the production of glucose increases both pre-prandial and post-prandial state. Inhibition of suppression of glucagon secretion and defective insulin release cause hyperglycemia by inducing the production of glucose excessively. As a result glucose levels during fasting increases and the body becomes unable to remove glucose from systemic circulation after food ingestion. When the blood sugar levels increase, metabolism activates pancreatic  $\beta$  cells by stimulating them constantly to start the secretion of insulin as a result of hyperglycemia. Since  $\beta$  cells encounter progressively increasing stress, the impairment of these cells resulted in apoptosis [Butler et al., 2003],[Ashcroft and Rorsman, 2012]. Physiological results of T2D show more deterioration due to insulin resistance and functional impairment of  $\beta$  cells. Deteriorated glucose uptake with over-production of liver sugar are observed in muscle and adipocytes. Because blood glucose cannot be regulated with insulin due to the insulin resistance and in spite of the fact that there is no need sugar, liver starts to produce sugar.

In adipocytes, the main reason of the damaged insulin-dependent glucose transport is the downregulation of the glucose transporters GLUT4. Under normal conditions, GLUT4 molecules are localized in the cytoplasm in the case of insulin absence. If the insulin receptors are stimulated by insulin so the insulin signaling is

activated. As a result, fusion of GLUT4 transporters inside to the cell membrane occurs and the glucose can be transported through these GLUT4 molecules [Chang et al., 2004]. In type 2 diabetes, glucose cannot be transported into the cells due to the lack of insulin. This situation causes high glucose level in blood for long periods and results in development of hyperglycemia [Sonksen and Sonksen, 2000].

### **2.3. Metabolic Inflammation**

Inflammation is also a factor in the development of obesity-related insulin resistance. In obese individuals, adipose tissue exhibits higher levels of macrophages compared with lean people [Weisberg et al., 2003]. Also the pro-inflammatory cytokine (IL-6 and TNF $\alpha$ ) production in the adipose tissue increases in insulin resistant and diabetic individuals. Besides, in obese rodents, suppression of TNF $\alpha$  results in the decrease of insulin resistance [Tajiri et al., 2005].

Increasing production of the pro-inflammatory cytokines recruit M1 macrophages known as “classically activated” into adipose tissue and thus provides activation of them. On the other hand, anti-inflammatory alternatively activated M2 macrophages are abundant in lean adipose tissue. M1 macrophages triggers the positive feedback which more increases the inflammation and insulin resistance by raising secretion levels of pro-inflammatory cytokines which decrease the insulin sensitivity [Olefsky and Glass, 2010].

### **2.4. Endocrine Function of Adipose Tissue**

As containing several types of cell like adipocytes, fibroblasts and immune cells, adipocytes secrete and release various secretory proteins named as adipokines into the circulating system. In obese humans and rodents, the production of adipokines are carried out by both visceral and subcutaneous adipocytes to mediate inflammation and insulin resistance. Adipokines are categorized into two groups; anti- and pro-inflammatory based on their inflammatory responses. While the levels of pro-inflammatory adipokines increase in obese humans and rodents, anti-inflammatory adipokine levels reduce.

Adipocytes, occupying the excess amount of cell population in the adipose tissue, supply the reversible overabundance energy storage. Excessive nutrition uptake causes adipocytes hypertrophy and hyperplasia which are the expansion of the cell volume and the increase of the cell number of the adipocytes, respectively. Expansion of the fat mass causes increased levels of fatty acid (FA) release and as a result of this, elevated FA concentrations are observed in obese people [Gordon, 1964].

Firstly, FAs have been known entirely as an energy source for the tissues. Then the role of FAs as endocrine factors was discovered. The hypothesis of Randle et al. is the obesity-related insulin resistance could be the consequence of the competition between elevated circulating levels of FAs and glucose for oxidation in insulin-responsive cells. With obesity and IR, excess FAs cause the activation of inflammatory pathways and impairment of insulin signalling. As pro-inflammatory cytokines released from adipocytes in the inflammation, the activation of some kinases for instance Jun kinase (JNK), inhibitor of nuclear factor- $\kappa$ B (NF- $\kappa$ B), I $\kappa$ B kinase (IKK), Protein kinase C (PKC) are carried out by these cytokines. These activated kinases inhibit insulin signaling by increasing the serine residue phosphorylation of insulin receptor substrates-1 (IRS-1) [Petersen and Shulman, 2006].

Nutrition overload causes adipocyte cells suffering from hypoxia which triggers the cell autonomous inflammation by releasing of metabolically active cell signalling proteins adipokines such as resistin, leptin and adiponectin. They attract the recruiting of pro-inflammatory macrophages into adipose tissue. Then these macrophages secrete cytokines to stimulate the activation of the inflammation in neighboring cells which increase the affect of inflammation and insulin resistance.

Addition of the adipokine production with inflammation in adipose tissues, some metabolic disorders related with obesity such as hyperlipidemia, endoplasmic reticulum (ER) stress, and hyperglycemia may cause insulin resistance which also affects peripheral tissues. Thus the activation of signalling cascades of inflammation can be triggered.

Leptin is an adipocyte-secreted pro-inflammatory adipokine which is expressed by *obese* gene and responsible for the regulation of feeding behavior. Any disruption of *ob* gene causes inhibition of leptin production which then result in overweight and obesity onset. While the leptin deficient mice (Lep<sup>ob</sup>/ Lep<sup>ob</sup>) showing hyperphagia, obesity and IR, exogenous leptin administration decreases obesity and IR. On the contrary to these studies, it has been displayed that plasma leptin levels increases in

obese individuals implying that obese subjects demonstrate leptin resistance which might be caused by impaired leptin transportation, ER stress and obesity-induced inflammation. Another roles of leptin are the regulation of gluconeogenesis and the fatty acid oxidation in muscle and liver [Kwon and Pessin, 2013].

Adiponectin is the important adipokine which circulates at highest level in bloodstream. Its main expression source is differentiated adipocytes. The best known role of adiponectin is regulating the insulin sensitivity. Contrary to leptin, the levels of adiponectin do not show any increment with obesity. Moreover, in obese people the adiponectin levels show inclination to decrease and in people with anorexia nervosa the adiponectin levels increased [Chandran et al., 2003],[Pannacciulli et al., 2003]. Adiponectin levels are importantly decreased in obese humans and rodents because pro-inflammatory factors including hypoxia, TNF $\alpha$ , IL-6 or ROS inhibit the adiponectin expression in adipocytes. Adiponectin also enhances AMPK activation for the glucose uptake and fatty acid oxidation in muscle and inhibition of gluconeogenesis in liver. The adiponectin deficiency in mice has been revealed that it causes high fat diet-induced inflammation and leads to insulin resistance while the mice with overexpressing adiponectin exhibit improvement of insulin sensitivity [Kwon and Pessin, 2013].

Resistin is a protein expressed by white adipocytes in rodents and adipose tissue macrophages in humans. Although the function of resistin is not explained clearly, serum resistin levels has a tendency to increase in the case of rodent obesity and continuous expression of resistin causes insulin resistance [Vidal and Orahilly, 2001]. It promotes insulin resistance by stimulating the expression of proinflammatory cytokines such as TNF $\alpha$  and IL-6.

Interleukin-6 (IL-6) and Tumor necrosis factor (TNF $\alpha$ ) are the pro-inflammatory cytokines that are secreted by adipose tissue and included in progression of obesity and insulin resistance [Fernandez and Ricart, 2003].

Expression of IL-6 displays a correlation with BMI and its expression increases by insulin and TNF $\alpha$ . In humans and rodents, peripheral application of this cytokine promotes insulin resistance, hyperglycemia and hyperlipidemia [Stith and Luo, 1994],[Petersen et al., 2004]. Insulin signalling impairment might be observed as IL-6 develops insulin resistance by decreasing the GLUT-4 and IRS-1 expression. [Rieusset et al., 2004]. The concentrations of plasma IL-6 increase also in patients with T2D. [Vozarova et al., 2001].

Studies have displayed that plasma TNF $\alpha$ , BMI and triacylglycerols are positively correlated with each other. It has been shown that the levels of TNF $\alpha$  in *ob/ob* mice adipose tissue elevated compared with wild-type controls [Schafer et al., 2001]. High levels of TNF $\alpha$  in WAT has been reported that TNF $\alpha$  is associated with the obesity and inflammation. TNF $\alpha$  also induces insulin resistance by promoting lipolysis, consequently increasing the FAs levels and decreasing the expression of GLUT-4 and IRS-1 [Fonseca et al., 2007]. In diet-induced obese mice, gene deletion of TNF $\alpha$  or its receptors protect mice from obesity-induced insulin resistance, partially [Uysal et al., 1997].

### 3. ENDOPLASMIC RETICULUM

Endoplasmic reticulum is firstly defined as a network comprising of membrane vesicles that are contiguous with nucleus found in eukaryotic cells [Palade, 1956]. This membranous network structure consisting of the tube-like structures and flattened sacs spreads throughout the cytoplasm and occupies almost half volume of the cell [Kaufman, 1999]. These sac-like network is called as cisternae and kept together by the cytoskeleton. It has a cisternal space enclosed by the phospholipid membranes which reaches to the nucleus and connects to the nuclear envelope.

Endoplasmic reticulum is a structurally and functionally complex organelle that is responsible for the synthesis, folding and the secretion of the proteins. Protein homeostasis which contains biosynthesis, folding, building up, modification, exportation and degradation of the proteins is regulated by ER [Ron and Walter, 2007], [Kaufman, 1999]. It also plays a major role in  $\text{Ca}^{2+}$  storage and regulates the  $\text{Ca}^{2+}$  homeostasis [Gorlach et al., 2006].

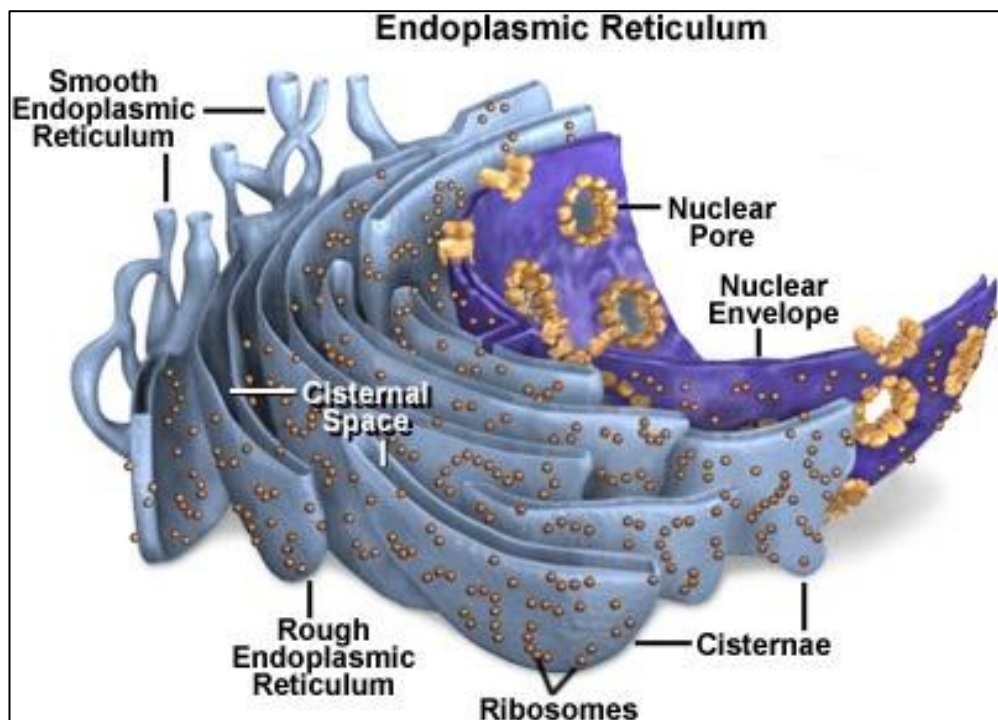


Figure 3.1: The structure of ER.

ER is observed as two sub-compartments called as rough ER (RER) and smooth ER (SER). The surface of the rough ER is ribosome-studded, while smooth ER is free of ribosomes. The abundance ratio of rough and smooth ER show difference among the cell types related with their functions. For instance, RER is rich in the cells specialized in secreting high amounts of protein, on the other hand, SER is outstanding in muscle cells, neurons, steroid synthesizing cells and hepatocytes. Smooth ER is distributed throughout the cytoplasm of the cells, whereas rough ER becomes dense around the nucleus and Golgi apparatus.

There are also morphological differences between the rough ER and smooth ER. RER has a granular like appearance because of the presence of ribosomes on its surface and sheet like domain, while SER has a curvature and tubular feature [Baumann and Walz, 2001]. The composition of membrane proteins show differences between RER and SER. However, general ER proteins are shared by both of them, various number of proteins that participate in the protein synthesis processing and translocation are enriched in rough ER [Kreibich et al., 1978]. Due to the protein translocation has a significant role, all cells must have RER. Only the single type of SER called transitional ER that involves in protein packaging for transportation to Golgi from the ER is also found in all cells [Palade, 1975].

The translation of the proteins starts in the cytosol. Ribosomes involving mRNAs are carried to the membrane of the ER. This recruitment occurs via signal sequences that contain Signal Recognition Particles (SRP) within the N-terminus of the newly synthesized polypeptides. Then the polypeptides are translocated to the lumen of the rough ER. The signal sequence is cleaved by peptidases in ER lumen. So the protein folding and the assembly process starts [Seiser, 2000]. After the vast majority of the cellular proteins enter the ER lumen from the translocons which involve various Sec proteins and cover the lipid bilayer. Then they undergo modifications, folding and the assembly. The oxidative environment of the ER lumen, chaperons and folding enzymes display compatible working for the proper folding and the assembly of the proteins [Helenius and Aebiz, 2004]. Proteins intrinsically tend to encounter several errors during folding process. Moreover, genetic mutations, toxic chemicals, errors originating from transcription or translation, cellular stresses for instance extreme temperature and osmotic pressure can endanger the folding rate and efficiency. So the conditions necessary for the efficient protein folding cannot be created in the cell [Bukau, 2006]. For this reason, ER develops some mechanisms to prevent the defects

during protein maturation. ER uses its quality control mechanism (ERQC) to prevent the accumulation of the misfolded or the unfolded proteins [Ellgaard and Helenius, 2003]. If the native conformation of the polypeptide is gained, it is sent to its target destination. If the folding is postponed or a defective conformation arises, the proteins are exposed to additional folding attempts or chosen for ER-associated degradation (ERAD) process [McCracken and Brodsky, 1996].

Disruption of the folding reactions or a raised demand for folding cause the formation of imbalance between the ER capacity and the recruited protein amount to the ER. When the capacity of the ER is exceeded, abnormal accumulation of the proteins in ER lumen triggers ER stress [Ron and Walter, 2007].

Several signalling pathways called as Unfolded Protein Response (UPR) are activated to deal with this stress. The cells take some precautions via UPR such as increasing of ER folding and modification capacity, reducing of the global protein synthesis, increasing of the synthesis of the chaperons and the activity of ERAD to become adaptive to the stress. If the ER stress becomes serious and chronic or if the UPR cannot restore the homeostasis in the ER, several signalling pathways triggering apoptosis are activated [Vembar and Brodsky, 2008].

## 4. ENDOPLASMIC RETIKULUM STRESS

Some of the various factors that play a significant role in protein folding are temperature, chaperons, lipid bilayer, salt concentration. The systemic adjustment of these factors are achieved by ER so the suitable environment for protein folding mechanism has been established [Anelli and Sitia, 2008]. After the proteins are folded into native conformation in ER, they are subjected to post-translational modifications such as N-linked glycosylation, disulfide bond formation, proteolytic cleavages, hydroxylation, oligomerization [Hubbard and Ivatt, 1981], [Fwell et al., 2001]. ER resident chaperons, foldases and lectins such as calreticulin and calnexin work together during protein folding and help folding mechanism to function efficiently. Any imbalance in the environment of the ER such as  $\text{Ca}^{2+}$  depletion, redox capacity changes, glucose deprivation, inhibition of N-linked glycosylation can cause ER stress. Protein folding mechanism can be affected adversely due to the sensitivity to such insults. These stresses induce the accumulation of the aggregated or misfolded proteins in the ER [Schroder, 2008].

The ER quality control mechanism work with folding pathways synchronously and permits solely properly folded proteins to be exported to the Golgi apparatus. Its selection ability becomes effective even in the presence of the minor disruptions in the folding efficiency. Incorrectly folded proteins are detected by ERQC, so the ER retains these polypeptides to accomplish the folding process or targets them for degradation mechanism called ERAD. Unsuccessful polypeptides in gaining their native conformation lead to accumulation of the misfolded proteins [Ellgaard, 1999]. Whenever the amount of the synthesized proteins in the cell exceed the folding capacity of ER and loading capacity of ERAD, unfolded proteins accumulate in the ER. This case is explained in thermodynamics as any conformational change resulted in having a higher free energy than native conformation is unfolded. Many conformation possibilities in which amino acid sequence plays a major role in the determination, exist for the proteins. Definitely, these conformations have free energy. Several folding attempts continues until the protein reaches to the conformation requiring the lowest free energy and the folding stops [Dobson et al., 1998]. In native proteins, the hydrophobic sites are hidden in the core of the protein. However, in non-native state, these hydrophobic sites remain on the surface and the contact with water

increases free surface energy. So these proteins form aggregates that cause the ER stress. As a response to ER stress, several signalling pathways called as unfolded-protein response (UPR) are activated in eukaryotic cells and this cellular stress is aimed to keep under control.

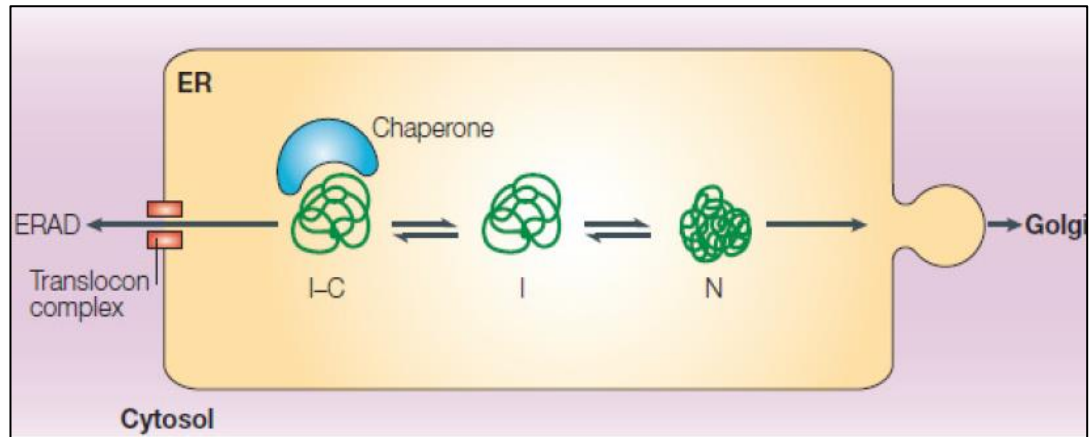


Figure 4.1: Transportation of native proteins to golgi and translocation of unfolded peptides to cytoplasm by ERAD (I:unfolded protein, N: native protein, I-C: Unfolded protein-chaperon complex).

## 5. UNFOLDED PROTEIN RESPONSE (UPR)

The major signalling pathways of UPR are activated via ER-resident protein sensors which are IRE1 $\alpha$ , PERK and ATF6. These proteins have cytosolic, transmembrane and ER-luminal domains. Unfolded protein detection is carried out by ER-luminal domain. Transmembrane domain targets the proteins through the ER membrane. Signal transmission is accomplished by the cytosolic domain [Ron and Walter, 2007],[Schroder and Kaufman, 2005].

ER-resident chaperone BiP is an important regulator for UPR pathways. It has an ATPase domain in N-terminus and substrate binding domain in C-terminus. Substrate binding domain provides the binding of BiP to the hydrophobic residues of unfolded proteins and ATPase domain assists the folding via changing the conformation by the help of ATP hydrolysis (Figure 5.1) [Zhang and Kaufman,2004]. In homeostatic states, these three protein sensors are retained inactive binding with ER chaperone BiP (Binding Immunoglobulin Protein) also known as GRP78. Under stress conditions, BiP dissociates from the stress sensors upon high levels of unfolded proteins to help protein folding. This release cause the activation of the signalling pathways [Bertolotti,2000].

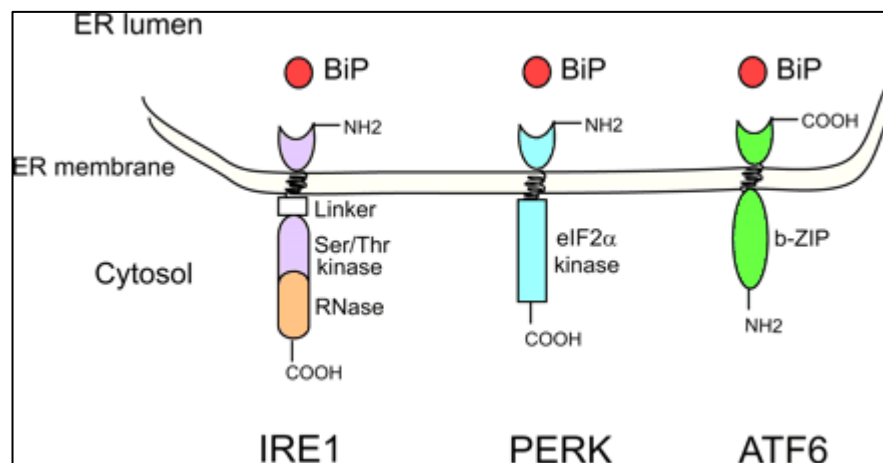


Figure 5.1: The general structure of the sensors in ER.

Sensor activation happens with the proteolytic cleavage of ATF6 and the homodimerization of PERK and IRE1. The main role of each signaling pathways is restoring the ER homeostasis by decreasing general translation while raising the ER

chaperones expression and ERAD activity. If the processes cannot be successful, the stress burdened on ER cannot be relieved then the apoptotic response will be started by these three signaling cascades.

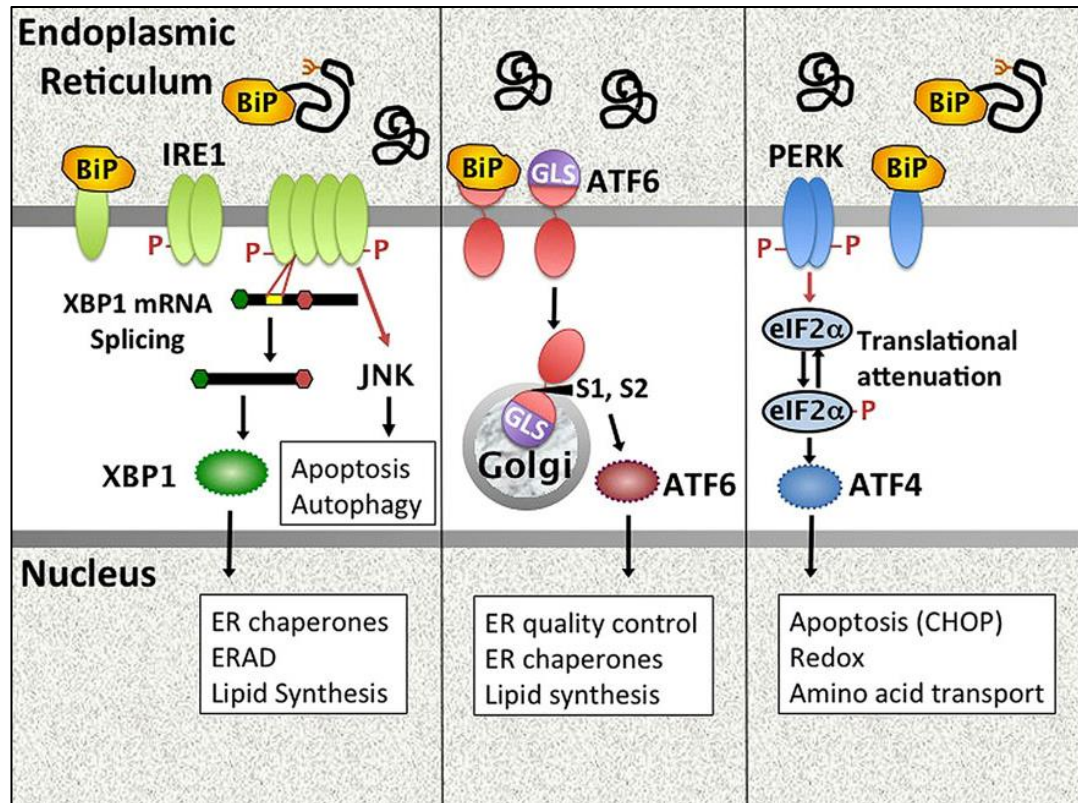


Figure 5.2: ER stress signaling pathways.

## 5.1. PERK Pathway

The most rapidly activated stress transducer branch of UPR is Protein kinase RNA-like endoplasmic reticulum kinase (PERK) pathway after ER stress exposure. It has a luminal and a cytosolic domain having protein serine/threonine kinase activity. When there is no stress, BiP is bound to luminal domain of PERK. Loss of this interaction occurs when the accumulation of the unfolded proteins increase in ER. Once released from BiP, PERK is autophosphorylated and dimerized. Phosphorylated state of PERK leads increasing its kinase activity and in turn it phosphorylates its direct substrate  $\alpha$  subunit of the eukaryotic translation initiation factor-2 (eIF2  $\alpha$ ) from serine51 residue whose phosphorylation is not based on nuclear transportation, transcription or translation process [Bertolotti,2000], [Harding et al.,1999].

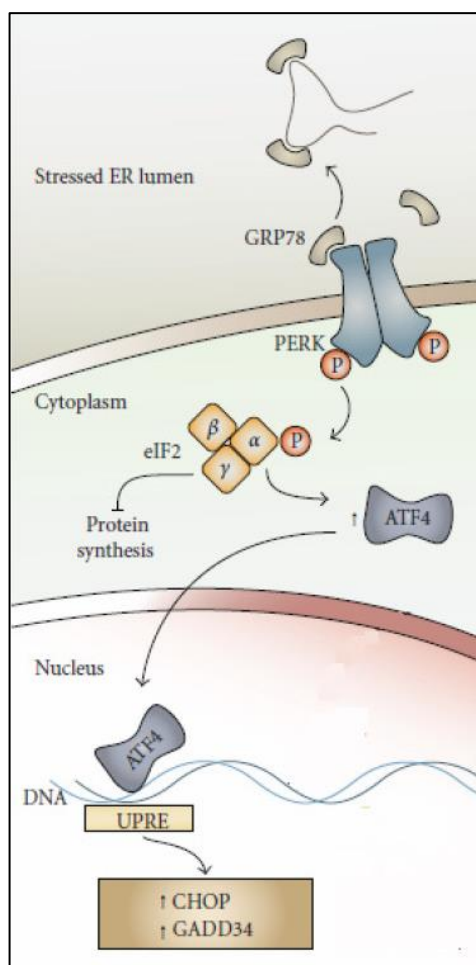


Figure 5.3: The formation of UPR signal by ER-stress activated PERK.

Therefore the synthesis of this protein is inhibited immediately after ER stress emerges. The completion of the eIF2  $\alpha$  phosphorylation and repression of the translation take 30 minutes after the initiation of ER stress [Novoa et al.,2003]. Phosphorylation of this factor prevents its capability to start translation of proteins. Thus, in the level of global protein synthesis decreases. eIF2 $\alpha$  phosphorylation also induces the expression of stress-induced transcription factors; CHOP and ATF4 [Scheuner et al., 2001]. Consequently, upon chronic ER stress, PERK behaves an inducer of apoptosis targeting the ATF4/CHOP pathway.

## 5.2. ATF6 Pathway

The third pathway of UPR is Activating Transcription Factor 6 (ATF 6). ATF6 contains three domains which are cytosolic domain at amino end, transmembrane

domain and the luminal domain at carboxyl end. The luminal domain involves localization signals. It is known that it has two isoforms ATF  $\alpha$  and ATF  $\beta$ . Under stress conditions, it is released from molecular chaperone BiP, and then it is transported to the Golgi apparatus by the localization signals. In Golgi, ATF 6 undergoes a proteolytic cleavage by the SP1 (Site-1 and then Site-2 Proteases (S1P and S2P, respectively)[Shen and Prywes, 2004].

The luminal domain is cleaved by S1P and N-terminal portion is cleaved by S2P. After the proteolytic cleavages the cytosolic N-terminal fragment which encodes a transcription factor called basic leucine zipper (bZIP) becomes free [Haze et al.,1999]. The translocation of N-terminal fragment to the nucleus and matching up with its consensus sequences occurs. Thus the transcription of related UPR genes for instance XBP1 [Yoshida et al., 2001], CHOP [Ma et al., 2002] and BiP [Yamamoto et al., 2004], are enhanced.

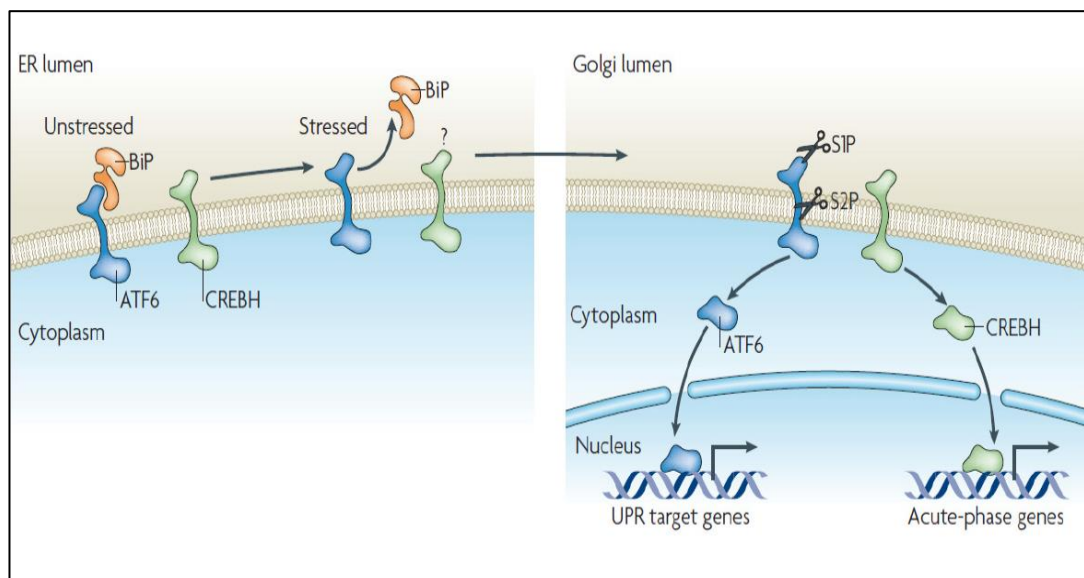


Figure 5.4: The formation of UPR signal by ER-stress activated ATF6.

### 5.3. IRE1 Pathway

The inositol-requiring enzyme-1 (IRE1) is the first discovered stress sensor and the most conserved part of UPR. It is an ER localized transmembrane protein involving stress sensor domain in N-terminus, a transmembrane domain and a cytosolic part that acts as both kinase and endoribonuclease activity.

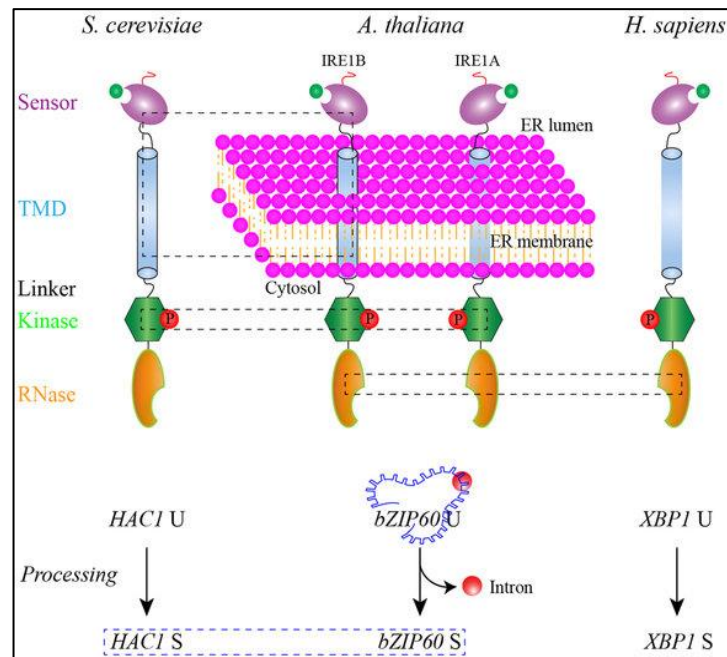


Figure 5.5: The structural profile of IRE1.

Two isoforms of IRE1, IRE1 $\alpha$  and IRE1 $\beta$  are encoded in mammals. The expression of IRE1 $\alpha$  is ubiquitous and embryonic lethality has been observed in IRE1 $\alpha$  knockout mice. On the other hand, the expression of IRE1 $\beta$  is restricted and IRE1 $\beta$  knockout mice could remain alive [Chen and Brandizzi, 2013].

The efficiency of IRE1 $\alpha$  to detect ER stress requires the release of BiP. Sensation of the ER stress and detection of the unfolded protein accumulation are accomplished by its N-terminal luminal domain which allows enzyme autoactivation. Triggering the UPR is carried through the cytoplasmic and RNase domain [Hetz et al., 2009], [Hetz et al., 2011]. The kinase activity of IRE1 is required for both activation of RNase and the transmission of the UPR signal arisen in ER. Upon ER stress, RNase of IRE1 is induced to be activated in consequence of conformational changes, autophosphorylation and oligomerization [Ali et al., 2011], [Korennykh et al., 2009]. IRE1 activation occurs by means of autophosphorylation which enables the opening of an active region. Opened region permits binding of nucleotides [Papa et al., 2003]. After binding, a conformational change is triggered for RNase domain of IRE1 to become activated. This conformational change might contain binding either ATP or ADP to the kinase domain. It has been shown that ADP is a more powerful activator *in vitro*, while ATP is enable of starting phosphorylation [Sidrauski and Walter, 1997]. Nucleotide binding to the kinase site promotes the cytosolic domain of IRE1 to be

dimerized [Lee et al., 2008b]. Consequently, active IRE1 splices Hac1, Xbp-1, bZIP60 mRNA in yeast, mammals and plants, respectively using its nuclease-like characteristic (Figure 5.5) [Zhang et al., 2016]. This cleavage results in a frame shift and thus extremely active transcription factor spliced Hac1, XBP1 and bZIP60 have been generated. The sXBP1 in mammals, organizes a lot of genes related with protein synthesis and folding, ER-associated degradation, autophagy, trafficking (Figure 5.6) [Walter and Ron, 2011].

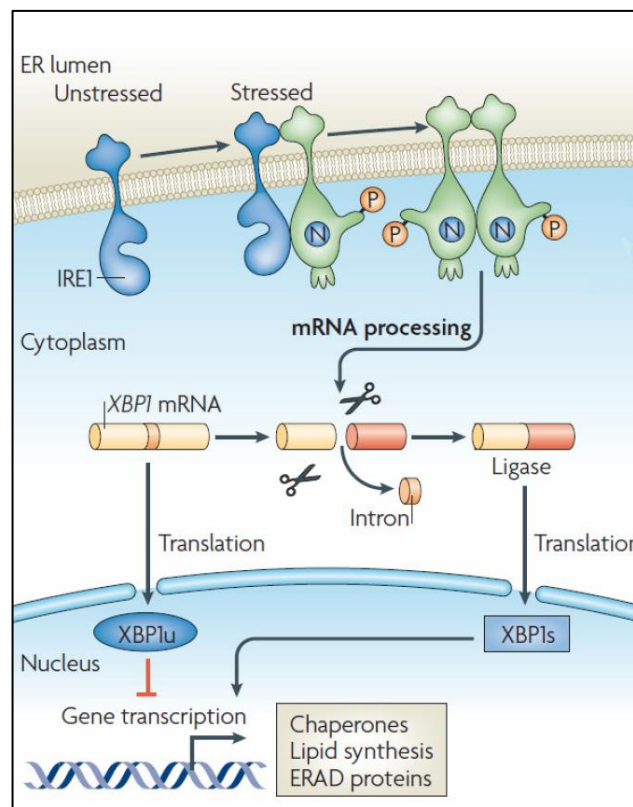


Figure 5.6: The formation of UPR signal by ER-stress activated IRE1.

### 5.3.1. IRE1 and Inflammatory Response

ER stress involves several pathological cases such as diabetes, atherosclerosis obesity, neurodegenerative diseases and inflammation. Reciprocal regulation between ER stress and inflammation has been discovered. ER stress is triggered by the proinflammatory stimuli such as TLR ligands or cytokines. In turn, inflammatory responses are initiated or amplified. All three UPR branches activate the main transcriptional regulator of pro-inflammatory pathways, nuclear factor- $\kappa$ B (NF- $\kappa$ B)

and activator protein 1 (AP1) pathways. Upon ER stress, a response is created by the formation of IRE1 $\alpha$  and TNF receptor-associated factor 2 (TRAF2) complex which leads the phosphorylation and degradation of I $\kappa$ B causing nuclear translocation of NF- $\kappa$ B. Besides, apoptosis signal-regulating kinase 1 (ASK1) is recruited by this IRE1 $\alpha$ -TRAF2 complex and leads the activation of JUN N-terminal kinase (JNK) which results in the increased expression levels of pro-inflammatory genes via increased activity of AP1 (Figure 5.7) [Wang and Kaufman, 2014].

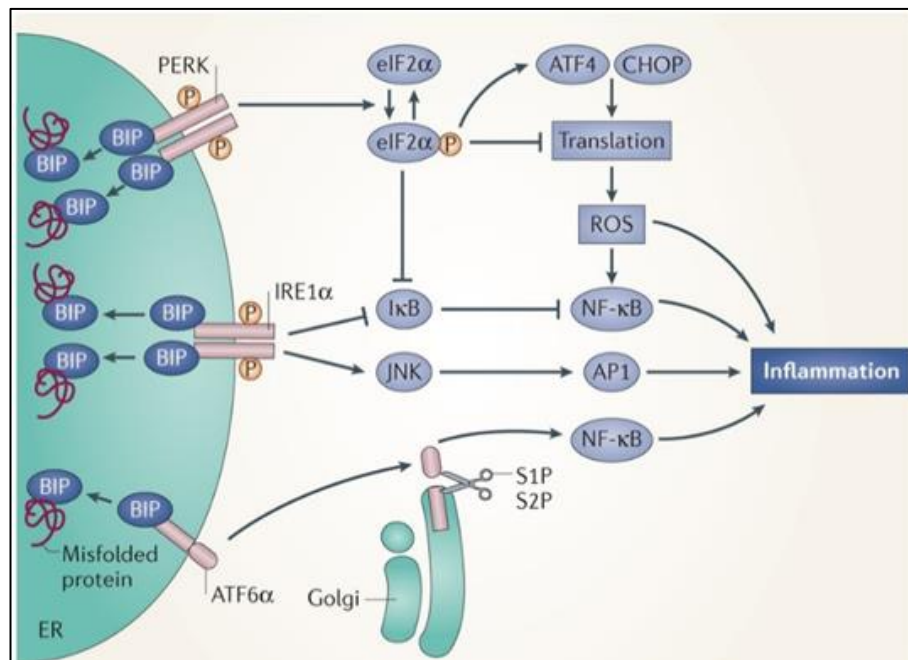


Figure 5.7: The unfolded protein response (UPR) and inflammation.

### 5.3.2. Regulated-IRE1 $\alpha$ -Dependent Decay (RIDD)

Upon ER stress, the cell fate is determined by IRE1 $\alpha$  either splicing or directing to RIDD which is Regulated-IRE1 Dependent Decay. In spite of the fact that, XBP-1 is known the only discovered splicing substrate of IRE1 $\alpha$ , several kinds of RNA are demonstrated as RIDD targets [Hollien et al., 2009],[Upton et al., 2012],[Han et al., 2009]. Even though the importance of RIDD substrates could not be explained clearly, some RIDD processes are severe to indicate the cell fate determination depends on IRE1 $\alpha$ . In the process of response for adaptation, IRE1 $\alpha$  directs RIDD to the mRNAs related with expression of ER-translocating proteins. Thus the further demand of protein folding in ER is restrained [Han et al., 2009]. To increase the protein folding

capacity, the splicing of XBP-1 mRNA is carried out by IRE1 $\alpha$  for the enhancement of quality-control factors of ER. If the ER homeostasis cannot be restored, IRE1 $\alpha$  stops the splicing of XBP-1. It also inhibits adaptive responses and triggers RIDD pathway for apoptosis [Upton et al., 2012], [Han et al., 2009].

The changeover from adaptation response to apoptosis occurs due to the increased level of ER stress resulting in degradation UPR target genes such as chaperone BiP [Han et al., 2009]. Whenever the intensity of ER stress approaches the threshold level, RIDD starts apoptosis by inhibiting the anti-apoptotic miRNAs. For the initiation of apoptosis, proapoptotic protease caspase-2 is necessary. Caspase-2 upregulation is the clue of the initiation of apoptosis. As a result, IRE1 $\alpha$  degrades the anti-caspase-2 factors and triggers apoptosis via induction of caspase-2 activity [Upton et al., 2012]. All these studies display that IRE1 $\alpha$  is a switch between the adaptative state and apoptosis [Lin et al., 2007], [Lin et al., 2009].

Tam et al. suggested that different mechanisms are carried out by activated IRE1 RNase for cleaving RIDD substrates or XBP1/HAC1 RNA. It has been considered that IRE1 oligomer formation is required for HAC1 or XBP1 mRNA splicing while the monomer or dimer IRE1 is indispensable for RIDD activity. Previous studies have revealed that R1039 residue in yeast is responsible for binding to HAC1 RNA [Korennykh et al., 2011]. The alteration of R1039 to Ala in yeast IRE1 reduced the RNase activity for HAC1 RNA, but it stayed active for cleavage of RIDD substrate BLOS1 showing that R1039 residue is only engaged in HAC1 RNA cleavage not for RIDD cleavage reaction [Tam et al, 2014].

Starting from this study, it was aimed to find out the mammalian homologous residue of yeast R1039 in IRE1 and a mutation will be performed in the investigated residue which is considered to be effective in the decrease of RNase activity of IRE1. Thus, survival pathway of IRE1 is aimed to be suppressed for XBP1 splicing, while the RIDD cleavage activity is aimed to be enhanced with the addition of ER stress agent thapsigargin. Upon ER stress, the adipokine secretion from adipocytes is initiated. The objective of our study is to investigate the effects of SIK2 on adipocyte secretome by ablating the XBP1 splicing activity of IRE1 but not RIDD under ER stress by qPCR.

Recent studies have shown that IRE1 connects with retinoic acid-inducible gene 1 (RIG-I) pathway by the generation of RNA ligands and in some circumstances activation of IRE1 can be triggered by some pathogens. A newly connection between

IRE1 $\alpha$  and inflammatory signalling including RIDD mechanism and antiviral RNA helicase RIG-I has been recently discovered. This pathway has been called as IRE1–RIDD–RIG-I. Retrotranslocation of some bacterial toxins to the ER may result in the interference with ER homeostasis. For instance, unfolded A1 subunits of cholera toxin in ER are detected by IRE1 sensor leading to its activation. Activated IRE1 triggers the RIDD pathway to produce single stranded mRNA fragments lacking 3' polyA-tails or 5'-caps which usually label cytosolic mRNA as “self”. RIDD cleaves the mRNAs that lack markers of self. The accumulation of these mRNA fragments make them favorable ligands for antiviral sensor RIG-I. Activation of RIG-I by Mitochondrial antiviral-signaling protein (MAVS) initiates an inflammatory response via the NF- $\kappa$ B and IFN pathways (Figure 5.8) [Lencer et al., 2015].

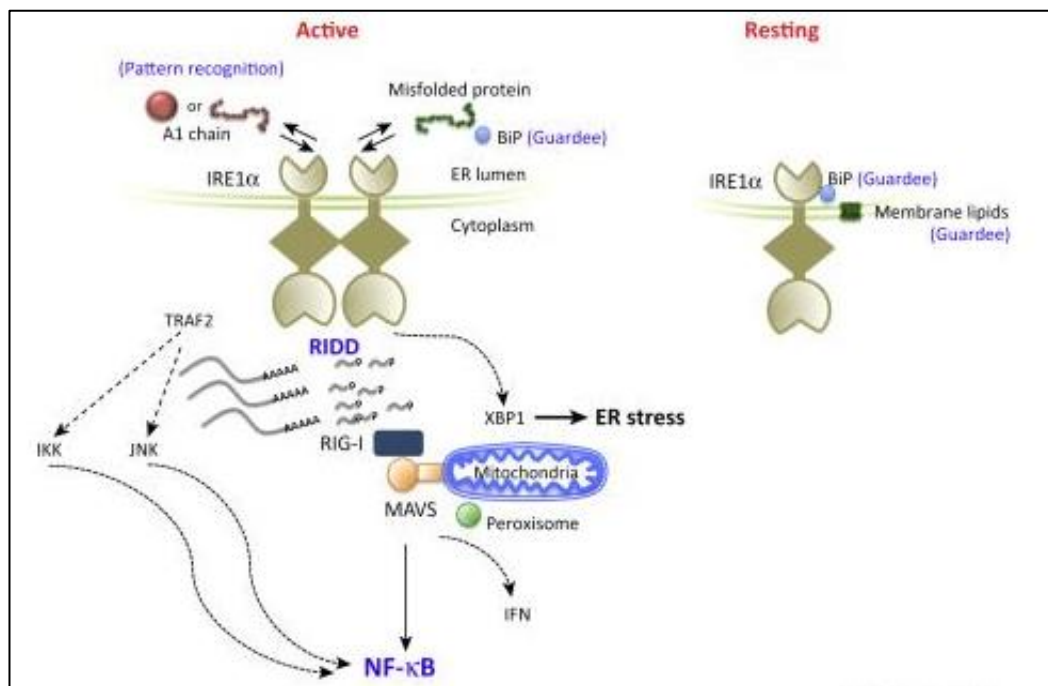


Figure 5.8: The IRE1–RIDD–RIG-I pathway.

Upon activation of UPR, generated RNA ligands are degraded by the RNA helicase SKIV2L resulting in the restriction of the RIG-I activation and prevention of inappropriate inflammatory responses. RIDD also degrades the mRNAs encoding tapasin which is a MHC class I antigen-processing molecule and essential for the maturation of the MHC class I molecules in the ER lumen. Antigen presentation is interfered with the degradation of tapasin and other molecules of MHC-I class. RIDD also functions in the degradation of some microRNAs such as miR-17. Upon chronic

ER stress, thioredoxin-interacting protein-TXNIP mRNA stability is increased by decreasing the levels of TXNIP destabilizing miR-17. High levels of TXNIP triggers the NLRP3 inflammasome causing the cleavage of Pro-Caspase 1 and then maturation and secretion of inflammatory cytokine IL-1 $\beta$ . Thus IRE1-TXNIP pathway is considered as the terminal UPR that causes the inflammation initiation and programmed cell death.

On the other hand, phosphorylated IRE1 $\alpha$  also serves as a docking site for TRAF2 (TNF receptor associated factor 2) and induce an inflammatory response by activating ASK/JNK or IKK-dependent pathways (Figure 5.9) [Janssens et al., 2014].

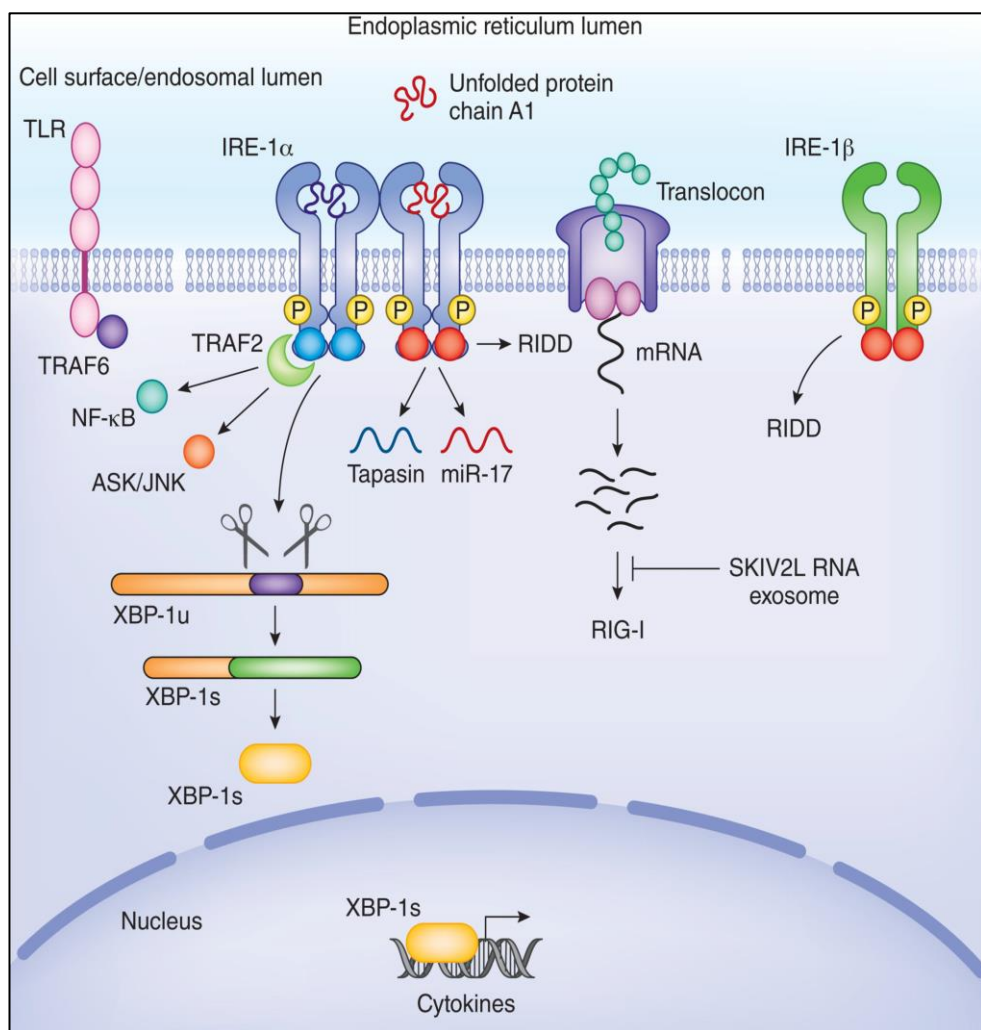


Figure 5.9: IRE1 intersects with inflammatory pathways.

When the phylogenetic tree of main species is examined, conserved functions are detected in immune responses with the evolution of UPR. IRE1-HAC1 branch in

most fungi has been conserved. However, absence of HAC1 gene in *S. Pombe* shows that activated IRE1 induces only RIDD pathway. Thus the ancestral function of IRE1 was considered as RIDD. While the IRE1 endonuclease of *S. Pombe* functions in RIDD (endonuclease domain shown as red), the IRE1 endonuclease of *S. Cerevisiae* functions in HAC-1 splicing (endonuclease domain shown as blue) (Figure 5.10) [Janssens et al., 2014].

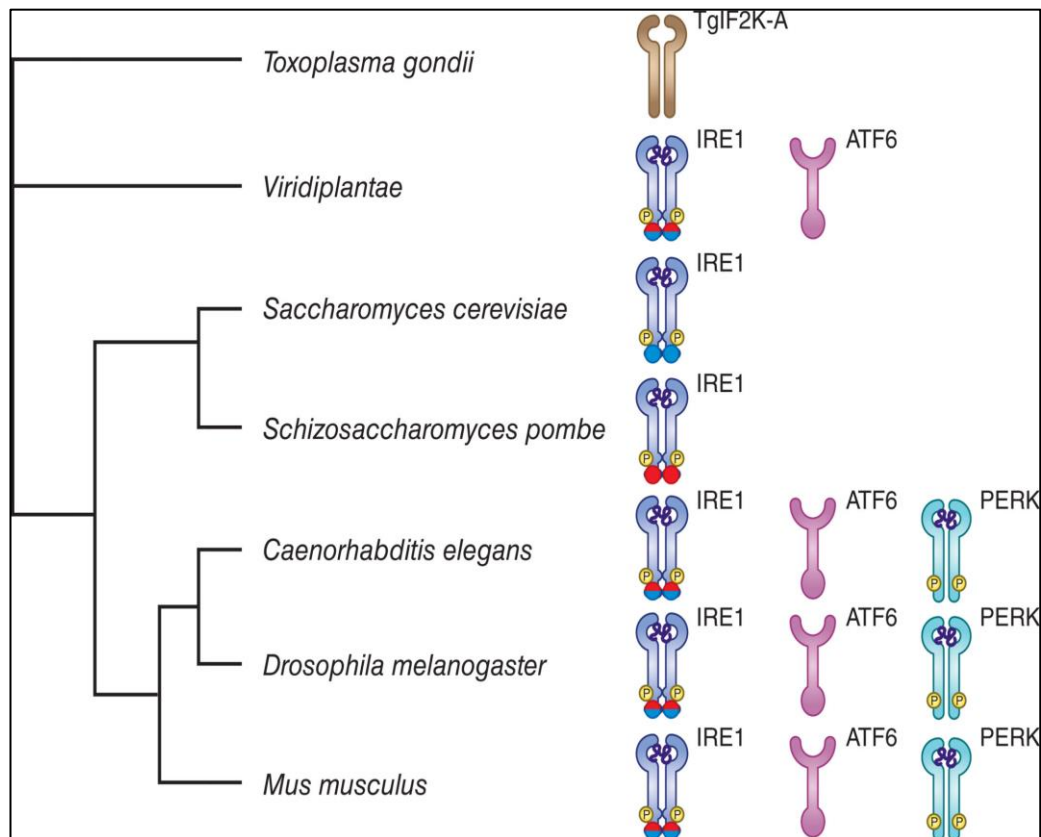


Figure 5.10: Evolution of the UPR shows conserved functions in immune responses.

In protozoa, expression of TgIF2K-A which is a transmembrane kinase provides the phosphorylation of eIF2 $\alpha$  in case of ER stress response due to the lack of orthologs of IRE1 and XBP. Thus the translational control can be carried out by this way.

In plants, ATF6 and IRE1-XBP1 branches are conserved and PERK is not present. In *A. Thaliana*, the splicing of bZIP60 the transcription factor is carried out by IRE1 and cleavage of transmembrane domain leads nuclear localization of bZIP60. In ATF6 pathway, cleavage of bZIP28 and bZIP17 are carried out in the case of ER stress by S1P and S2P and the BiP is induced to start ER stress response. The absence of the translational regulation by PERK has been compensated for RIDD mechanism.

UPR activation is not restricted with the protein overloading into the ER, it is activated with the abiotic stress such as heat shock or salt stress. Also, the activation of IRE1 and bZIP60 is enhanced in response to pathogen and antibacterial defense.

In *C.elegans*, the three branches of UPR are conserved and they function for the protection against devastating hyperinflammatory reactions. The IRE1-XBP-1 is activated in response to infection and it is required for survival in the presence of pathogens. The infection cannot be controlled by XBP-1 but it is rather required to decrease destructive effect of an innate immune response on ER homeostasis. This shows the IRE1-XBP-1 branch is evolutionarily-conserved because of the protection against toxicity in ER created by inflammatory response.

In mice and humans, fully establishment of three UPR sensors provides the interaction with inflammatory response pathways according to inflammation levels [Janssens et al., 2014].

## 6. SALT-INDUCIBLE KINASE FAMILY

Salt-inducible kinase (SIK) was the Serine/Threonine kinase belongs to AMP-activated protein kinase (AMPK) family. It was first identified in the adrenal glands of rats treated with high-salt diet and named as SIK1. Consequent studies enable the discovery of the two additional isoforms of SIK, named as SIK2 and SIK3. In mammals, the mRNA levels of SIK1 is extremely high in skeletal muscle, brain, testis and adrenal glands whereas its level is lower in heart, liver and adipose tissue [Horike et al., 2003]. On the other hand, SIK2 is expressed in liver, adipose tissue and brain abundantly while SIK3 mRNA expression is seen in all tissues (Figure 6.1) [Katoh et al., 2004].

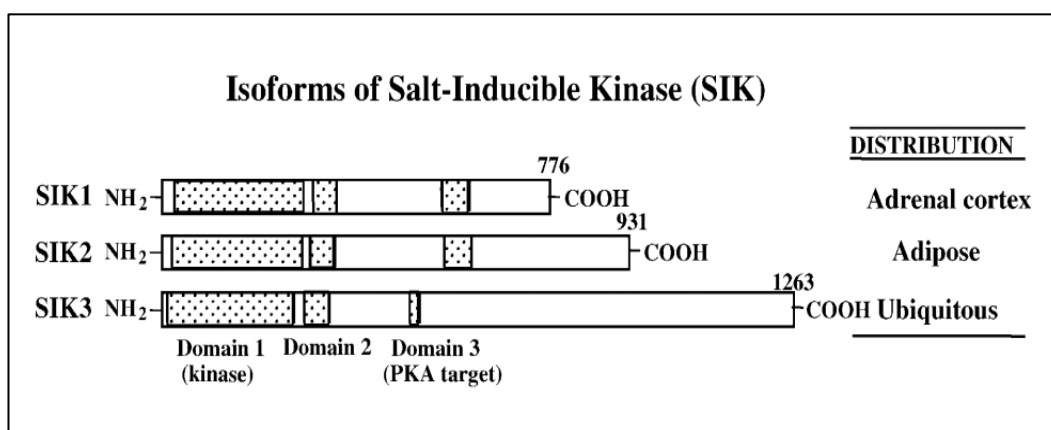


Figure 6.1: The isoforms of Salt-Inducible Kinase.

The kinase domains of the proteins that are related to AMPK family display sequence homology and the activation of all are carried out by liver kinase B1 (LKB1) [Manning G., 2002], [Lizcano JM., 2004]. Thus SIK proteins have also a highly conserved kinase domains at their N-terminus due to be considered as member of AMPK family. An ubiquitin-associated (UBA) domain exist adjacent to its kinase domain. Moreover, in all SIK isoforms, there exists a Protein Kinase A (PKA) phosphorylation region in C-terminal domain from which the activation of the proteins controlled. These regions are considered as nucleus localization signals (NLS) so the phosphorylation by PKA allows the transportation of SIK from cytoplasm to nucleus [Katoh et al., 2004]. It has been claimed that the raising activity of SIKs depends on the kinase domain phosphorylation by LKB1.

Another phosphorylation region in SIK is the serine 358 residue which is phosphorylated by AKT also known as Protein Kinase B. (PKB) Hence SIK is activated for the insulin signaling pathways [Berdeaux, 2011].

## **6.1. SIK2**

SIK2, the subfamily of salt-inducible kinase found in homo sapiens, is a 130 kDa protein consisting 926 amino acid containing kinase domain between 20-271 residues and UBA domain between 295-553 residues (UNIPROT, Q9H0K1). SIK2 shows high similar sequence ratio with the other isoforms.

It takes part in energy metabolism and regulation of the gene expression as a response to the effects of hormones and nutrients. SIK2 also plays a role in different pathways such as lipogenesis, insulin signaling, gluconeogenesis.

### **6.1.1. SIK2 and Insulin Sensitivity**

Insulin is a hormone which retains the blood glucose at normal levels via regulating the protein, lipid and carbohydrate metabolism by rendering the glucose diffusion from blood to the fat, muscle and liver cells. In these cells, glycogenesis; conversion of glucose to glycogen or lipogenesis; conversion of glucose into the fats occurs. High levels of insulin restricts the liver to produce and excrete the glucose into blood. Thus, by increasing the lipogenesis as well as decreasing the glycogenesis, insulin maintains the normal blood glucose levels [Sonksen and Sonksen, 2000]. The reduction in responsiveness of the tissues to the normal concentration of insulin is defined as insulin resistance which is the main characteristic of obesity and type 2 diabetes. The occurrence of insulin resistance in such metabolic diseases brings to mind the relation of insulin signalling pathways with glycogenesis and lipogenesis.

When circulating insulin levels increases in the blood, insulin interacts with its receptor found on the cell surface. Insulin receptor (IR) is a tyrosine kinase and the binding of insulin to the insulin receptor results in IRS1 phosphorylation which enhances the activation of downstream signaling mechanism. The kinase activity of insulin receptor is activated via autophosphorylation of the Tyrosine residues, then activated IRS-1 plays a significant role activating the phosphoinositide 3-kinase

(PI3K) pathway which is the important signal transducer in the cell. It activates the several pathways for the regulation of the glucose uptake. Eventually, the role of IRS-1 in insulin signalling and lipogenesis is important [Katoh et al., 2004].

SIK2 displays higher expression levels in hepatocytes and adipocytes [Katoh Y., 2002]. It is plentiful in both white and brown adipocytes and during adipogenesis, upregulation of SIK2 can be observed in pre-adipocytes [Horike N., 2003]. Following studies have demonstrated that diabetic mice show an increase in SIK2 expression and activity in their white adipose tissue.

Whether the SIK2 has a role in the regulation of the insulin signaling mechanism in the adipocytes is a issue of concern. Depending on the studies which display high expression level of SIK2 in mature adipocytes, it is considered whether its substrates are phosphorylated in insulin exposed adipocytes. As a result, the phosphorylation of IRS-1 by SIK2 was discovered. IRS 1 (insulin receptor substrate-1), the firstly discovered substrate of SIK2, is a significant modulator in insulin signaling pathway. Its phosphorylation occurs at Ser794 in humans and at Ser798 in rats [Horike et al., 2003], [Katoh et al., 2004]. It is declared that the phosphorylation of IRS1 from Ser794 is related with the decrease of insulin signalling [Gual et al., 2005]. Serine phosphorylation results in inefficient participation in the insulin signaling which then force adipocytes to become insulin resistant. Insulin resistant rats proved this case by showing a higher level of phosphorylated Ser794 of IRS 1.

After all, SIK2 is considered as an important factor in the regulation of insulin signalling and may be the causative element in development of T2D [Horike et al., 2003].

### **6.1.2. SIK2 and Inflammatory Response**

According to recent studies, it has been demonstrated that SIKs are the major molecular switches whose inhibition has an effect on the reprogramming of macrophages to an anti-inflammatory state. Inhibition of SIK2 promotes the anti-inflammatory state during the macrophage differentiation with the high level of anti-inflammatory cytokine production such as IL-10 and low level of proinflammatory cytokine production such as TNF $\alpha$ .

In macrophages, TLR stimulation creates a response that follows the phosphorylation and activation of CREB which is regulated by protein kinases Mitogen- and Stress-Activated Protein Kinase (MSK) 1/2. CREB-Regulated Transcription Co-activator (CRTC) can enhance the activity of CREB. Under normal conditions, phosphorylation of CRTCs by AMP-Activated Protein Kinase (AMPK)-related kinase family provides binding regions for 14-3-3 proteins. The complexes of CRTC-14-3-3 are restrained in the cytosol thus the activity of CREB is remained low. The stimuli that can desphosphorylate the CRTCs cause the disruption of the CRTC-14-3-3 complex which triggers their migration into the nucleus. As a consequence an interaction between CREB and CRTC can be created in the nucleus.

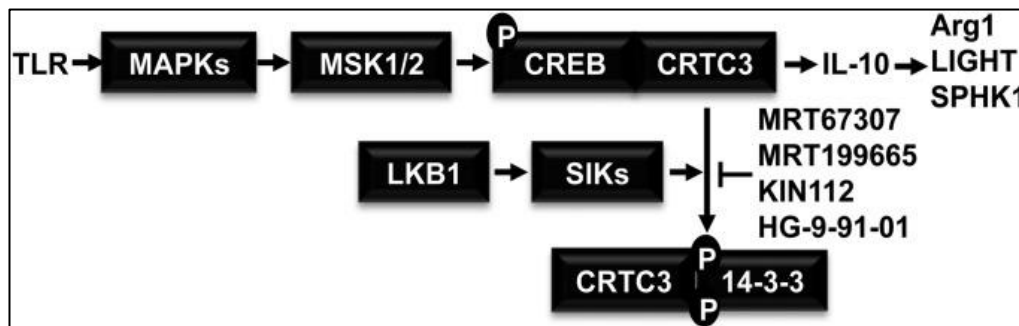


Figure 6.2: The regulation of IL-10 production by LKB1-SIK-CRTC3.

Recent studies have revealed that SIK2 in macrophages phosphorylate CRTC3 and thus suppress the formation of regulatory macrophages which cause the production of IL-10 and other anti-inflammatory molecules. Inhibition of SIK2 cause the dephosphorylation of CRTC3 resulting in the migration to the nucleus where it enhances CREB-dependent gene transcription involving IL-10 production. It causes the formation of the anti-inflammatory state with the enhanced expression of regulatory macrophages such as ARG1, LIGHT and SPHK1 (Figure 6.2).

Based on these findings, the outstanding effects of SIK2 inhibitors on macrophage polarization imply an opportunity to treat the inflammatory and autoimmune diseases by developing drugs which target these kinases [Darling et al., 2016], [Clark et al., 2012].

### **6.1.3. The Relation Between SIK2 and p97/VCP Mediated ERAD**

p97/VCP (valosin-containing protein) is the member of type II AAA (ATPases associated with diverse cellular activities) proteins involving two ATPase domains. The ATPase activity is necessary for different cellular functions for instance regulation of transcription, response to DNA damages, control of cell cycle, autophagy and ERAD [Patel and Latterich,1998], [Wang et al.,2004].

Concurrently with ERAD activity, the role of p97/VCP is the removal of proteins from ER and direction them to proteasomal degradation mechanism resident in cytosol [Ye et al., 2003], [Ye et al., 2004]. This mechanism is important in regulating ER homeostasis by elimination of unfolded or misfolded proteins accumulated in the ER [Hampton, 2002], [Hoppe et al., 2000]. Recent studies has revealed that p97/VCP is a critical factor between ubiquitin-proteasome and autophagy.

SIK2 plays a significant role in diminishing the ER stress effects by facilitating ERAD. The activity of SIK2 is essential for the translocation of the misfolded proteins from ER for ERAD. Additionally, SIK2 is the unique member of the AMP-activated protein kinase family which interacts with the ATPase of p97/valosin-containing protein (VCP). SIK2 induces the ATPase activity of p97/VCP via phosphorylating its Ser-770 residue. The activation of p97/VCP allows ubiquitinated proteins to be transported from ER lumen to cytosol for degradation by ERAD machinery. Recent studies have shown that SIK2 overexpression (SIK2-WT) provides increased ATPase activity of p97/VCP while SIK2 with kinase dead domain (SIK2-KD) does not increase the activity of p97/VCP. As a result, besides the interaction of SIK2 with p97/VCP, the kinase activity of SIK2 is critical for effective translocation of ERAD substrates [Yang et al., 2013].

## 7. MATERIALS

### 7.1. Cell Lines and Plasmids

In this study, LiSa-2 (from University of Ulm) and Hek293FT (ATCC) cell lines were used. pLenti-III-HA-IRE1<sup>WT</sup> and pLenti-III-HA-SIK2<sup>WT</sup> plasmids were obtained from Boğaziçi University, pLenti-III-HA-IRE1<sup>K888A</sup> construct was generated in our lab.

### 7.2. Chemicals

Dulbecco's Modified Eagle Medium-DMEM (Lonza, BE12-604F), Dulbecco's Modified Eagle Medium Ham's F-12 (Lonza, BE12-719F), Fetal Bovine Serum (Biowest, S181G-500), Penicillin streptomycin (P/S) (Pan Bio, P06-07100), 10X PBS (Lonza, BE17-517Q), 10X Trypsin – EDTA (Pan Biotech, P10-019100), Non fat dried milk powder (AppliChem, A0830), Genopure Plasmid Midi Kit (Roche, 03143414001), Genopure Plasmid Maxi Kit (Roche, 03143422001), Qiagen Plasmid Midi Kit (Qiagen, 12143), IRE1 $\alpha$  Antibody (Cell Signaling, 3294),  $\beta$ -Actin Antibody (Santa Cruz, sc-47778), 20X LumiGLO Reagent and 20X Peroxidase (ECL) (Cell Signaling, 7003), TurboFect Transfection Reagent (Thermo Fisher Scientific, R0531), Pierce BCA Protein Assay Kit (Thermo Fisher Scientific, 23227), DMSO (Sigma-Aldrich, D5879), Methanol (Sigma-Aldrich, 34885), Isopropanol (Merck, 109634), Ethanol (Absolute) (Sigma, 32221), APS (AppliChem, A1142), TEMED (AppliChem, A1148), Acrylamide Bis Solution %30 (Intron, IBS-BA004), Bisacrylamide (%40 Acrylamide) (Fisher BioReagents, 132836), Anti-Mouse Secondary Antibody (Cell Signaling, 7076), Anti-Rabbit Secondary Antibody (Cell Signaling, 7074), Bovine Serum Albumin (BSA) (Santa Cruz, sc-2323), Kanamycin Sulfate Biochemica (AppliChem, A1493), Agarose (Sigma, A9539), Glycine (SantaCruz, sc-29096), EDTA (AppliChem, A1103), Glycerol (Multicell, 800-040-EL), Sodium Chloride (AppliChem, A4661), HCl (Merck, 100314), Acetic Acid (Riedel de Hein, 27225), %37 Formaldehyde (J.T.Baker, 7041) Beta Mercaptoethanol (Appllichem, A1108), Hexadimethrine bromide (Polybrene) (Sigma, H9268), Aprotinin (AppliChem,

A2132), PMSF (AppliChem, A0999), SDS (Merck, 8220501000), Sodium hydroxide pellets (AppliChem, A3910), Sodium orthovanadate ( $\text{Na}_3\text{VO}_4$ ) (Sigma, S6508), Tris (Ultra Pure) (MP, 819623), Trypan Blue (Sigma-Aldrich, T8154), Tween20 (AppliChem, A1389), EGTA (AppliChem, A0878), Zinc chloride (AppliChem, A6285), Lentifectin Transfection Reagent (ABM, G074), Tryptone (Biolife, 171230), Yeast extract (Biolife, 160430), Agar Bios Special LL (Biolife, 180130), Puromycin (Sigma-Aldrich, P8833), Thapsigargin (Santa Cruz, sc-24017A)

### 7.3. Solutions

10X SDS- Running Buffer: 30,3 g Tris Base, 144,1 g Glycine and 10 g SDS are dissolved in 1 L distilled water. It is diluted to 1X when it will be used.

10X Transfer Buffer: 30,3 g Tris base and 144,1 g Glycine are dissolved in 1 L distilled water. When it will be used it is diluted to 1X with %10 10X Transfer buffer, %20 Methanol and %70 distilled water.

1X PBS: 10X PBS is diluted with distilled water to 1:10.

1X Trypsin: 10X Trypsin is diluted to 1X using 1X PBS.

10X TBS: 24,2 g Tris Base and 88 g NaCl are dissolved in 1 L distilled water.

1X TBS-T: 10X TBS is diluted with distilled water to 1:10 and %0,1 Tween 20 is added into it.

4X SDS Loading Dye: 0,2 M Tris-HCl (pH 6,8), %8 SDS, %40 Glycerol, %4  $\beta$ -mercaptoethanol, 50 mM EDTA ve %0,08 Bromophenol blue (BPB) are dissolved in water and stored at  $-20^\circ\text{C}$ .

LB Broth: 5 g Tryptone, 2,5 g Yeast Extract and 5 g NaCl are dissolved in water and then autoclaved to be sterile.

%5 Membrane Blocking Solution: %5 Non-fat dried milk powder is dissolved in 1X TBS-T.

10X TAE: 48,4 g Tris Base, 11,42 g ml acetic acid and 20 ml 0.5 M EDTA are dissolved in distilled water. It is diluted to 1X when it will be used.

0,5 M EDTA pH:8.0 :36,5 g EDTA is dissolved in distilled water. NaOH pellets are used to adjust pH to 8.0. Water is added up to 250 ml.

Lysis Buffer: 50 mM HEPES, 150 mM NaCl, 1mM EDTA, 1 mM EGTA, %10(v/v) Glycerol, %1 (v/v) Triton-X-100, 25 mM NaF, 10  $\mu\text{M}$   $\text{ZnCl}_2$  are dissolved

in desired volume of distilled water. The pH of solution is adjusted to 7.5 with HCl and stored at +4°C. When it will be used 10µg/ml aprotinin, 5µg/ml leupeptin, 1mM Na<sub>3</sub>VO<sub>4</sub>, 1 mM PMSF are added to lysis buffer solution.

LB Broth: 5 g Tryptone, 2,5 g yeast extract and 5 g NaCl were dissolved in 500 mL dH<sub>2</sub>O. After autoclaving it was used.

LB Agar: 1 g Tryptone, 0,5 g yeast extract, 1 g NaCl and 1,5 g BactoAgar were dissolved in 100 mL dH<sub>2</sub>O. After autoclaving it was used.

1 mM Thapsigargin (THA): 1 mg THA was dissolved in 1,54 ml DMSO and stored at -20°C.

## 7.4. Kits

Site-Directed Mutagenesis, RNA isolation, cDNA synthesis and quantitative Real-Time PCR experiments were performed using the following kits.

Table 7.1: Kits used.

Q5 Site-Directed Mutagenesis Kit	NEB
NucleoSpin RNA Mini Kit	MACHEREY-NAGEL
Dynamo cDNA Reverse Synthesis Kit	Thermo Scientific
Maxima SYBR Green qPCR Master Mix (2X)	Thermo Scientific

## 7.5. Equipments

Table 7.2: Equipments used.

CO <sub>2</sub> Incubator	Binder
Laminar Flow Cabinet	Clean Air
Water Bath	Memmert
Plate Reader	Thermo, Varioskan Flash
Fluorescent Microscope	Nikon Eclipse Ti
Electrophoresis and Transfer System	BioRad Mini Protean
Microcentrifuge	Beckman Coulter 22R
Centrifuge	Beckman Coulter, Allegra X-22
Real Time Thermal Cycler	Roche, LC480II
Shaker	Finepcr, BAE07
1,5 ml and 2 ml centrifuge tubes	Axygen
15 ml and 50 ml centrifuge tubes	CAPP
0,2 µm and 0,45 µm filter tips	TPP
pH meter	Mettler Toledo
Cell culture flasks and cryotubes	TPP
Glass Materials	Isolab
Vortex	Finepcr
-80°C Freezer	Symphany
Gel Imaging System	BioRad, ChemiDoc XRS+
Liquid Nitrogen Tank	Arpege 140
Pipettor	Gilson
Micropipettor	Gilson, Thermo
Filtered and non-filtered Micropipette Tips	CAPP
Pasteur Pipette	Isolab
Serologic Pipette	CAPP
Heat Block	VWR
Magnetic Stirrer	Scilogex
Thermal Cycler	BioRad
PVDF Membrane (0,45µM)	Merck Millipore, IPVH00010

## **8. METHODS**

### **8.1. Cell Culture and Passaging**

LiSa-2 cells were maintained in DMEM/F12 (Dulbecco's Modified Eagle Medium/Ham's F12) mixture medium supplemented with 10% Fetal Bovine Serum and 1% Penicillin/Streptomycin. The medium was refreshed every 2 days. The cells were preserved in the 37°C incubator with humidified atmosphere of 5% CO<sub>2</sub>.

Cell culture materials were pre-warmed to 37°C in waterbath before use. The cells were passaged before they reach 80% confluency. After the medium in the plate was removed by the vacuum, the cells were washed with 1X PBS twice. To detach the cell-to-cell and cell-to-surface attachment, 1X trypsin-EDTA was added onto the cells and incubated for 5 minutes in the incubator. The trypsin was neutralized with 2-fold volume of fresh culture medium. The cells were collected to the centrifuge tube with serological pipette. The cells were centrifuged at 1000 rpm for 5 minutes. The supernatant was removed and the cell pellet was dissolved in fresh medium. The cells were seeded drop by drop to the new petri dishes in diluted conditions.

### **8.2. Freezing of Cells**

After the cells reached 80% confluency were trypsinized and neutralized with media, they were centrifuged at 1000 rpm for 5 minutes. The pellet was dissolved in 10% DMSO containing growth medium and transferred to the cryotubes. The tubes were stored in -80°C and for long-term storage they were transferred to the vapor phase liquid nitrogen tank next day.

### **8.3. Defrosting of Cells**

The cryotubes taken from liquid nitrogen tank or -80°C were defrosted quickly in 37°C waterbath. Defrosted cells were transferred to the centrifuge tube containing fresh medium and centrifuged at 1000 rpm for 5 minutes. The pellet was dissolved in medium and seeded into the petri dishes.

## 8.4. Protein Isolation, BCA, Protein Preparation

Protein isolation is the process of breaking down the cell membrane with cell lysis buffer and various protease inhibitors and purifying the proteins from cell remnants. Inhibitors are used to avoid damaging the proteins. For isolation, the medium on the cells was removed by vacuum and the cells were washed with non-sterile ice-cold PBS twice. After that, freshly prepared cell lysis buffer containing aprotinin, PMSF, leupeptin and  $\text{Na}_3\text{VO}_4$  was added on the cells. The cells were disrupted by scraper on the ice. Homogenate was transferred to the eppendorf tubes and centrifuged at 14000 rpm  $+4^\circ\text{C}$  for 15 minutes. After centrifugation, the supernatant was transferred to a clean tube and stored at  $-20^\circ\text{C}$ .

BCA (Bicinchoninic acid Protein Assay) is a method to measure the concentration of the isolated proteins. For this technique, Thermo Fisher Scientific BCA Protein Assay Kit was used. BCA Reagent A and B in the kit was mixed at a ratio of 50:1 and 200  $\mu\text{l}$  of this mixture was added to the each well of the 96 well plate. 25  $\mu\text{l}$  of each protein sample or BCA standard replicate were added to the wells. BCA standards were prepared from bovine serum albumin at different concentrations (2mg/mL, 1,5mg/mL, 1mg/mL, 0,5mg/mL, 0,25mg/mL, 0,125mg/mL) to obtain the slope graphic. In Varioskan Flash device, the plate was incubated at  $37^\circ\text{C}$  and dark conditions for 30 minutes for the reaction. Then the OD measurement was done at 562 nm. The average of the replicates of the proteins were calculated and the slope graphic was plotted using the standards. The concentration of the samples were calculated according to the  $R^2$  value and the graphic equation in unit of  $\mu\text{g/mL}$ .

Making the proteins ready for loading to the gel by mixing them with 4X SDS Loading dye, after the concentration of the proteins were calculated by using the graphic obtained from BCA. At desired amount of the proteins were taken and mixed with loading dye at a ratio of 3:1. Then they were incubated at  $95^\circ\text{C}$  for 5 minutes to be denatured. They were ready for loading to the gel. These prepared samples can be stored at  $-20^\circ\text{C}$  at least two months.

## 8.5. SDS-PAGE and Western Blotting

SDS-PAGE is a technique of the separation of proteins based on size and charge. Western Blotting is transferring the separated proteins pattern onto a membrane and the detection of the presence, absence or expression level of a protein using an related antibody.

For this technique, polyacrylamide gels were prepared and the denatured proteins were loaded into the wells of the gel. The proteins were run at 80 V during the stacking gel and when they reached to the separating gel, it was run at 120 V until the bromophenol blue dye reach at the bottom of the gel.

Table 8.1: The solutions used for preparation of gels.

Separating Gel (10%)		Stacking Gel (4%)	
dH <sub>2</sub> O	3,9 mL	dH <sub>2</sub> O	4,35 mL
Tris-HCl (1,5M pH:8,8)	2,6 mL	Tris-HCl (1M pH:6,8)	750 µl
10% SDS	100 µl	10% SDS	60 µl
30% Acrylamide	3,3 mL	30% Acrylamide	800 µl
10% APS	100 µl	10% APS	30 µl
TEMED	10 µl	TEMED	6 µl

After the electrophoresis run finished, the proteins on the gel were transferred to the methanol-activated PVDF membrane and transfer step was done at +4° C, 100V for 2 hours. After the transfer step was completed, the gel was controlled by staining with Coomassie Brilliant Blue dye. Blocking of the non-specific binding was achieved by putting the membrane in the 5% non-fat dried milk powder in 1X TBS-T for an hour at room temperature. After blocking, the primary antibody suitable to the desired protein was prepared in 5% BSA in 1X TBS-T at stated ratio according to the activity of the antibody. The membranes were left on the shaker O/N at +4° C. After 16 hours, membranes were rinsed with 1X TBS-T 3 times. Then the membranes were exposed to the related secondary antibody prepared in 5% non-fat dried milk powder in 1X TBS-T and shaken at room temperature for 2 hours. Then the membranes were rinsed 3 times with 1X TBS-T. During rinsing, ECL solution was diluted to 1X and then the

images of the membranes were taken by help of ECL solution in BioRad ChemiDoc XRS+ device.

## **8.6. Transformation**

It was done to integrate the desired gene to be amplified into the bacterial genome. DH5 $\alpha$  cells were used as competent bacteria. According to the each plasmid number to be transformed, 25  $\mu$ l competent bacteria were transferred to the tubes. Related DNA was added into the tubes. They were incubated on ice for 10 minutes. Heat shock was done at 42 °C for 50 seconds. For cool shock, they were kept on ice for 1 minute. 500  $\mu$ l LB Broth containing non-antibiotic was added into the tubes. They were shaken on the shaker adjusted to 37 °C at 250 rpm for 1,5 hours. The bacteria were seeded on the agar plates. They were remained upside down and incubated O/N at 37 °C. After incubation, bacteria grown agar plates were stored at +4 °C.

## **8.7. Plasmid Isolation**

Roche Genopure Maxi Plasmid Kit was used for isolation. The bacteria grown in 200 mL LB Broth were divided into 50 mL falcons and centrifuged at 4000 rpm, +4 °C for 20 minutes. The supernatant was removed and RNase added suspension buffer was added totally 12 mL. The pellet was mixed to be homogenous and the homogenate was collected in one falcon. 12 mL lysis buffer was added onto it and it was inverted 6-8 times gently. It was incubated at room temperature for 2-3 minutes. 12 mL pre-cooled neutralization buffer was added to the mixture and it was inverted 6-8 times gently. It was incubated on ice for 5 minutes. Then the suspension was centrifuged at 4000 rpm, 4 °C for 20 minutes. During centrifugation, the filtered columns were activated with equilibration buffer. The supernatant obtained from centrifugation was filtered from columns and the column was allowed to empty by gravity flow. The plasmid remained at the filter was washed with 16 mL wash buffer twice. Then the column was transferred to a new falcon and 15 mL pre-warmed elution buffer was added. The column was allowed to empty by gravity flow. 1 mL isopropanol was added on the eluted plasmid and it was centrifuged at 4000 rpm, +4 °C for 1 hour and

15 minutes. Supernatant was discarded and 4 mL pre-cooled 70% ethanol was added and it was centrifuged at 4000 rpm, +4 °C for 30 minutes. Ethanol was discarded and the plasmid was allowed to dry. Then the pellet was dissolved in 100 µl Nuclease Free Water or TE Buffer and stored at -20 °C.

## 8.8. Lentiviral Transfection

Lentiviral transfection was used to make stable cell lines. The lentiviral vectors that have puromycin resistance gene were used as selectable marker. When the antibiotics were added to the medium, the cells that did not incorporate the vector, were killed off and the survival cells created stable cell lines. In LiSa-2 cells, the overexpression of IRE1 gene (IRE1-WT) and the mutant of the RNase domain (IRE1<sup>K888A</sup>) were generated by the lentiviral particles. It was controlled whether the transfection was successful by GFP given to the cells randomly. For this procedure, HEK-293FT cells were seeded 60% on the day before the transfection. Following day, IRE1-WT and IRE1<sup>K888A</sup> plasmids were given to the cells by the help of transfection reagent lentifectin. The cells were allowed to produce lentivirus for 24 hours. For transduction, the supernatant containing virus was collected and centrifuged at 500 g for 3 minutes. It was filtered with 0,45 µm filter and divided to the LiSa-2 cells which were passaged previous day. 8 µg/mL polybrene was added to the cells. Fresh growth medium was added to the HEK-293FT cells to repeat this step. After 24 hours, the medium of the plates which were done transduction was changed with fresh medium. The virus adding protocol was repeated at night. Next morning, the medium of the LiSa-2 cells were refreshed. After 48-72 hours, cells were treated with 1 µg/mL puromycin. This selection could be continued up to 7 days. In the end, the survival cells could generate stable cell lines.

## 8.9. Transient Transfection

For this procedure, LiSa-2 GFP, LiSa-2 IRE1-WT and LiSa-2 IRE1<sup>K888A</sup> cells were seeded 70-80 % on the day before the transfection. The plasmid concentration and the transfection reagent amount was calculated according to the plates to be used as indicated in the producer's protocol. Following day, HA and SIK2-WT plasmids

were given to the cells by transfection reagent turbofect. After 7-8 hours, the medium of the plate was changed with growth medium. The transfection duration was adjusted as 48 hours.

## 8.10. Site Directed Mutagenesis

To demonstrate the effect of the RNase activity of human IRE1 $\alpha$ , a mutation within RNase domain was done using Q5 Site-Directed Mutagenesis Kit. pLenti-III-HA-IRE1<sup>WT</sup> plasmid was used to construct stable cell line. The primers were designed of which Alanine was substituted to at position Lysine888. The following set of primers were used; forward: AGACCTGCGTgcATTCAGGACCTATAAAG, reverse : GTCTGGAGGGGGACAGTG. The product was verified by sequencing with reverse primer of pLenti-HA plasmid because the mutation site was localized at the end of the sequence. Thus, pLenti-III-HA-IRE1<sup>K888A</sup> mutant has been generated.

Table 8.2: Components for PCR.

Component	20 $\mu$ l Reaction	Final Concentration
Q5 Hot Start High-Fidelity 2X Master Mix	10 $\mu$ l	1X
10 $\mu$ M Forward Primer	0.75 $\mu$ l	0.5 $\mu$ M
10 $\mu$ M Reverse Primer	0.75 $\mu$ l	0.5 $\mu$ M
Template DNA	0.5 $\mu$ l	50 ng
Nuclease-free water	8 $\mu$ l	

Table 8.3: Cycling conditions of PCR Program.

Step	Temperature	Time
Initial Denaturation	98 °C	30 seconds
25 Cycles	98 °C	10 seconds
	69 °C	20 seconds
	72 °C	5,5 minutes
Final Extension	72 °C	2 minutes
Hold	4 °C	Hold

Table 8.4: Kinase, Ligase and DpnI (KLD) Reaction.

Component	Volume	Final Concentration
PCR Product	1 $\mu$ l	
2X KLD Reaction Buffer	5 $\mu$ l	1X
10X KLD Enzyme Mix	1 $\mu$ l	1X
Nuclease-free water	3 $\mu$ l	

For transformation, 5  $\mu$ l of KLD mix was added to 50  $\mu$ l of component cells. It was incubated for 30 minutes on ice. Heat shock was done at 42°C for 30 seconds. Then it was incubated on ice for 5 minutes. 950  $\mu$ l SOC outgrowth medium was added and it was shaken at 37 °C for 1 hour. 100  $\mu$ l was spread onto Kanamycin (+) plate and it was incubated overnight at 37 °C.

## 8.11. RNA Isolation

The cultured cells were trypsinized and collected by centrifugation. Then the cell pellets were lysed by adding 350  $\mu$ L Buffer RA1 and 3.5  $\mu$ L  $\beta$ -mercaptoethanol. They were vortexed vigorously. The mixture was applied into the NucleoSpin Filter placed in a 2 mL collection tube and centrifuged at 11000xg for 1 min. The filters were discarded, 350  $\mu$ L 70% ethanol was added to the lysate and mixed by pipetting up and down for 5 times. The lysates were loaded to the NucleoSpin RNA columns and centrifuged at 11000xg for 30 s. The columns were placed in new collection tubes, the lysates were pipetted up and down 2-3 times and loaded to the columns. They were centrifuged at 11000xg for 30 s. The columns were placed in new 2 mL collection tubes. 350  $\mu$ L MDB (Membrane Desalting Buffer) was added and centrifuged at 11000xg for 1 min to dry the membrane. DNase reaction mixture was prepared; for each isolation, 10  $\mu$ L reconstituted rDNase was added to 90  $\mu$ L reaction buffer for rDNase. 95  $\mu$ L DNase reaction mixture was applied onto the center of the column and incubated at room temperature for 15 min. 200  $\mu$ L Buffer RAW2 was added to the columns and centrifuged at 11000xg for 30 s. The columns were placed into new 2 mL collection tubes. 600  $\mu$ L Buffer RA3 was added to the columns and centrifuged at 11000xg for 30 s. The flow-through was discarded and 250  $\mu$ L Buffer RA3 was added to the columns and centrifuged at 11000xg for 2 min. The columns were placed into

nuclease-free collection tubes. The RNA was eluted in 60  $\mu\text{L}$  RNase-free  $\text{H}_2\text{O}$  and centrifuged at 11000xg for 1 min.

## 8.12. cDNA Synthesis

The isolated RNAs were used for cDNA synthesis. The cDNA synthesis was performed using minimum 200 ng RNA according to the protocol indicated in Table 8.5 with Dynamo cDNA Reverse Synthesis Kit and the PCR program in Table 8.6, cDNAs were diluted with 30  $\mu\text{L}$  RNase-free water and kept in  $-20^\circ\text{C}$  until quantitative real-time PCR (qPCR) analysis.

Table 8.5: Components for cDNA Synthesis from isolated RNA.

Component	Amount (20 $\mu\text{L}$ total)
10X RT Buffer	10 $\mu\text{L}$
Random Hexamer Primer Set	1 $\mu\text{L}$
M-MuLV RNase H <sup>+</sup> reverse transcriptase	2 $\mu\text{L}$
RNase-free $\text{H}_2\text{O}$	1-4 $\mu\text{L}$
Template RNA (min 200 ng)	3-6 $\mu\text{L}$

Table 8.6: PCR Program for cDNA Synthesis.

Temperature	Duration
25 $^\circ\text{C}$	10 minutes
37 $^\circ\text{C}$	60 minutes
85 $^\circ\text{C}$	5 minutes
4 $^\circ\text{C}$	Hold

## 8.13. Quantitative Real-Time PCR

After cDNA synthesis, the qPCR analysis was performed for LiSa-2 GFP, IRE1-WT and IRE1<sup>K888A</sup> using Thermo Scientific's Maxima SYBR Green qPCR Master Mix (2X). 9  $\mu\text{L}$  of Master Mix (SYBR Green qPCR Master Mix + Forward/Reverse Primers + NFW) and 1  $\mu\text{L}$  of diluted cDNA were put into each well. Ct values of

different genes were analyzed with two replicates. For housekeeping gene, RPLP0 was used and RPLP0's Ct values were subtracted from the Ct values of the related genes so  $\Delta\text{Ct}$  values of all genes were calculated. The  $\Delta\Delta\text{Ct}$  values were calculated using the average  $\Delta\text{Ct}$  value of the control cells which were transfected with their backbone HA plasmid for each gene. The foldchanges were calculated according to  $2^{-\Delta\Delta\text{Ct}}$  method. The foldchanges of gene expression were normalized to HA plasmid transfected cells so their gene expression foldchange was set to 1. P values were calculated according to Two-Way ANOVA. The experiments were repeated as two independent experiments.

## 9. RESULTS

### 9.1. Investigation of Mammalian Homologous Residue of yIRE1 R1039

Firstly, the alignments of the human IRE1 ERN1 gene (977 aa) and the *Saccharomyces cerevisiae* IRE1 gene (1115 aa) sequences were obtained from UniProtKB. Then the protein blast was performed between them. The mammalian homologous residue of yeast IRE1 R1039 was investigated as K888.

The protein codes, 3LJ0 for yIRE1 and 3P23 for hIRE1 were obtained from RCSB protein data bank. Then the crystal structures of the superimposed forms of these two proteins were shown using Swiss-PDBViewer. The superimposed forms of the LYS888 of hIRE1 and ARG1039 of yIRE1 were shown in Figure 9.1. The structural change of the K888 residue of hIRE1 was shown in the case of mutation of which Alanine was substituted at this position (Figure 9.2). The reason of selecting Alanine to substitute for Lysine888 was to remove the effects of the side chain of Lysine. This mutation truncated the side chain at the  $\beta$ -Carbon atom. Thus the involvement of side chain interactions could be measured.

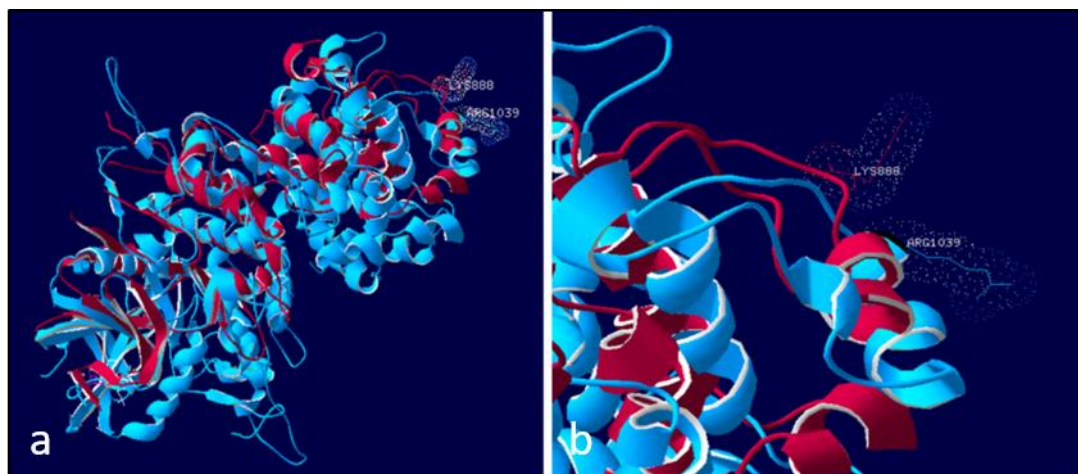


Figure 9.1: The crystal structures of the superimposed forms of yIRE1 (blue) and hIRE1 (claret red). a) Full image. b) The zoomed version of the image.

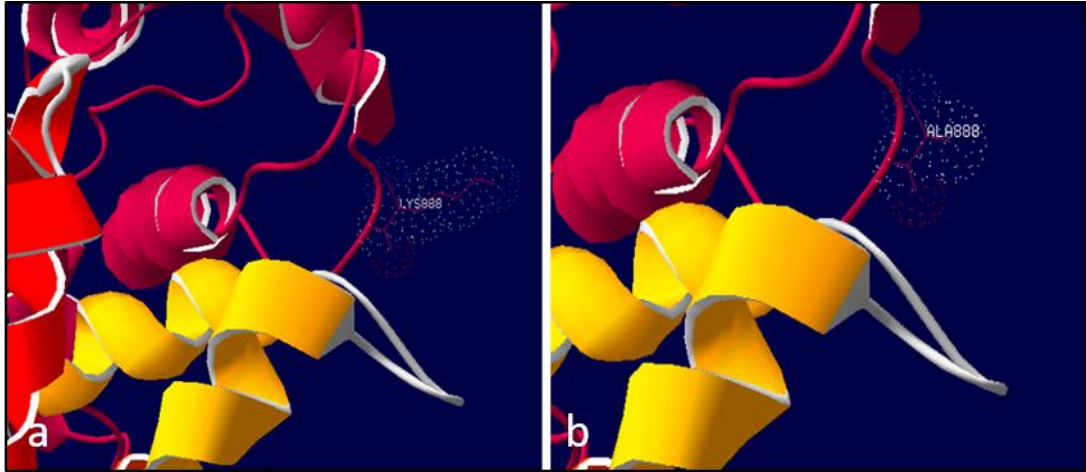


Figure 9.2: The structure of hIRE1 after the mutation changing Lysine to Alanine. a) The structure of LYS888 residue in hIRE1. b) The structure of ALA888 residue in hIRE1.

## 9.2. Confirmation of IRE1<sup>K888A</sup> Mutant Product by Sequencing

The mutation was done within RNase domain of human IRE1 by substituting Alanine at position Lysine888. The lentiviral vector pLenti-III-HA-IRE1<sup>WT</sup> was used as backbone vector for mutagenesis (Figure 9.3).

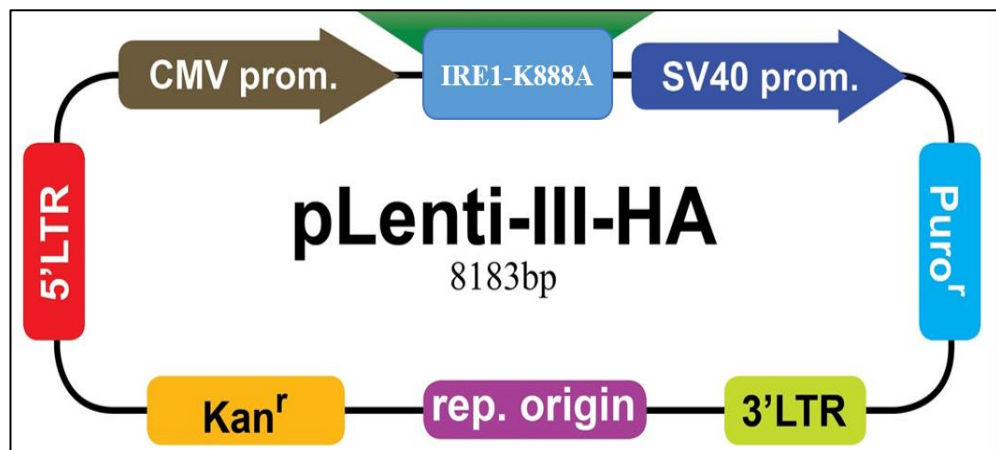


Figure 9.3: The p-Lenti-III-HA vector backbone map.

The product was then confirmed by sequencing. Due to the end-localization in sequence, the mutation was verified using the reverse primer of pLenti-HA plasmid.

According to the sequencing result, AAA (Lysine) was converted to GCA (Alanine) shown in red circle (Figure 9.4).

```

hIRE1_gene          GAGCCGTGGTGAAGATGGACTGGCGGGAGAACATCACTGTCCCCCTCCAG
170110-057_C20_19ACBAB001-46 GAGCCGTGGTGAAGATGGACTGGCGGGAGAACATCACTGTCCCCCTCCAG
*****

hIRE1_gene          ACAGACCTGCGTAAATCAGGACCTATAAAGGTGGTTCTGTCAGAGATCT
170110-057_C20_19ACBAB001-46 ACAGACCTGCGTGCATCAGGACCTATAAAGGTGGTTCTGTCAGAGATCT
*****

hIRE1_gene          CCTCCGAGCCATGAGAAATAAGAAGCACCCTACCGGGAGCTGCCTGCAG
170110-057_C20_19ACBAB001-46 CCTCCGAGCCATGAGAAATAAGAAGCACCCTACCGGGAGCTGCCTGCAG
*****

hIRE1_gene          AGGTGCGGGAGACGCTGGGGTCCCTCCCCGACGACTTCGTGTGCTACTTC
170110-057_C20_19ACBAB001-46 AGGTGCGGGAGACGCTGGGGTCCCTCCCCGACGACTTCGTGTGCTACTTC
*****

```

Figure 9.4: The part of the sequence showing the mutated residue of hIRE1.

### 9.3. Generation of the Stable Cell Lines of GFP, IRE1-WT and IRE1<sup>K888A</sup> in LiSa-2 Cells

In this experiment; lentiviral transfection was performed to generate stable LiSa-2 GFP, IRE1-WT and IRE1<sup>K888A</sup> cell lines. For this protocol, these three plasmids were given to the HEK-293FT cells via transfection. The cells were allowed to produce related lentiviruses for 24 hours. Then HEK-293FT medium containing the produced lentiviruses were given to the LiSa-2 cells with the help of the polybrene. After 48-72 hours, antibiotic selection was initiated with the concentration of 1 µg/mL puromycin which was determined by performing puromycin killing curve on LiSa-2 cells before. Puromycin-resistant stable cell lines were generated in 7 days. Randomly given GFP plasmid was used as a control group for the other stable cell lines. After second passage, puromycin-resistant LiSa-2 cells were lysed and protein samples of each group were collected. The IRE1 protein levels of transfected cells were compared to wild-type LiSa-2 with Western Blot. While the endogenous IRE1 level in LiSa-2 WT has shown a slight band, the bands in IRE1-WT and IRE1<sup>K888A</sup> groups have confirmed that the overexpression of IRE1 was achieved successfully. The IRE1 level in GFP cells has shown 3 folds higher expression compared to LiSa-2 WT cells. It was

detected that the expressions of IRE1 in IRE1-WT and IRE1<sup>K888A</sup> cell lines were 17 and 21 folds higher than the control group of LiSa-2 GFP cells, respectively (Figure 9.5).

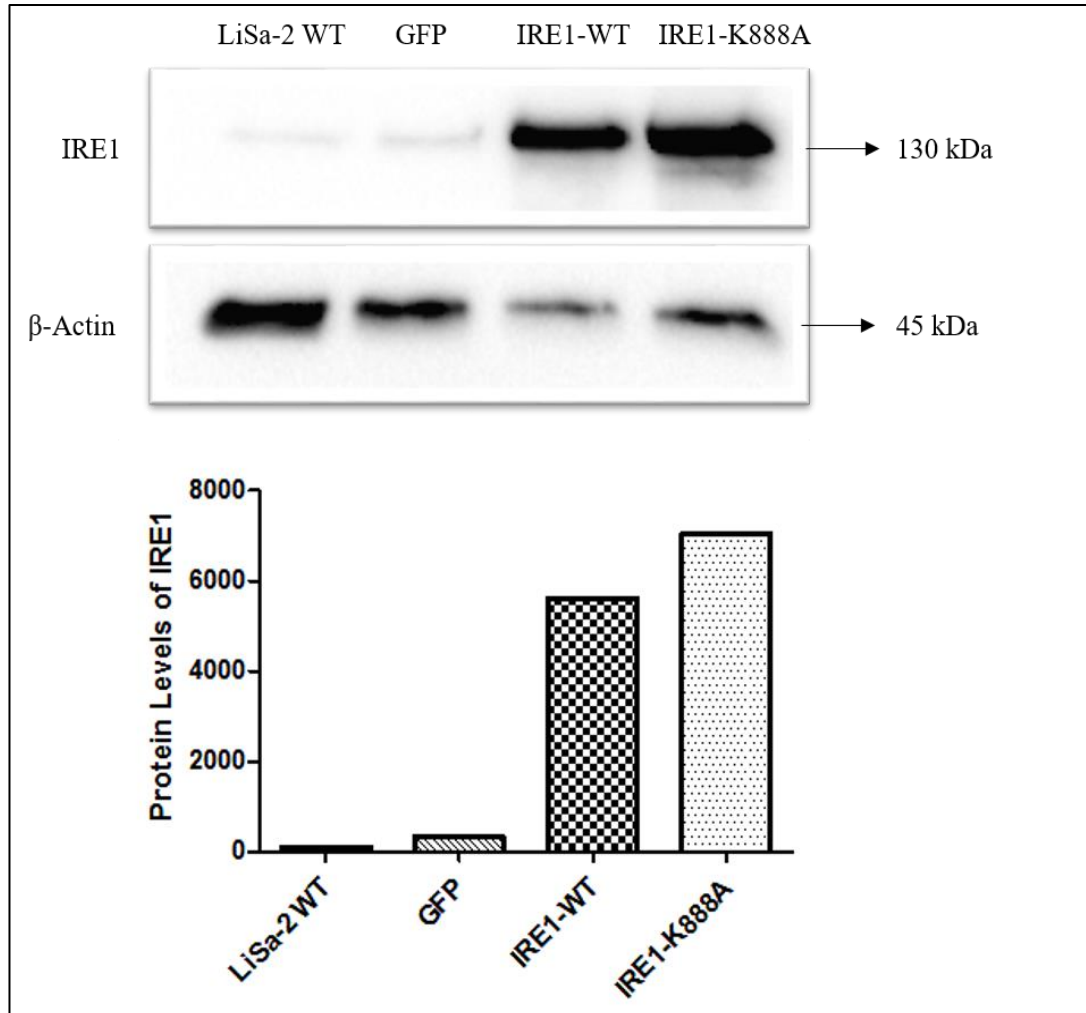


Figure 9.5: Confirmation of IRE1 overexpression with Western Blot.

#### 9.4. Gene Expression Levels of LiSa-2 GFP and IRE1-WT Stable Cell Lines

In this experiment, LiSa-2 GFP and LiSa-2 IRE1-WT cells were seeded 70-80 % confluency. Following day, these cells were transiently transfected with HA and SIK2-WT plasmids separately. HA plasmid was given to the cells because the backbone vectors of these cell lines were p-Lenti-III-HA. Transfection duration was determined as 48 hours so 24 hours after transfection, 1  $\mu$ M Thapsigargin treatment was applied to one set of the cells to create ER stress. After 24 hours of incubation

with Tha, both groups which were treated and non-treated with Tha, were collected for the RNA isolation. After RNA isolation, cDNA synthesis and then q-PCR were performed. The values acquired from their backbone vector HA plasmid were subtracted from the values obtained from LiSa-2 GFP and IRE1-WT (with or without Tha treatment). So the effects of the HA plasmid have been canceled out.

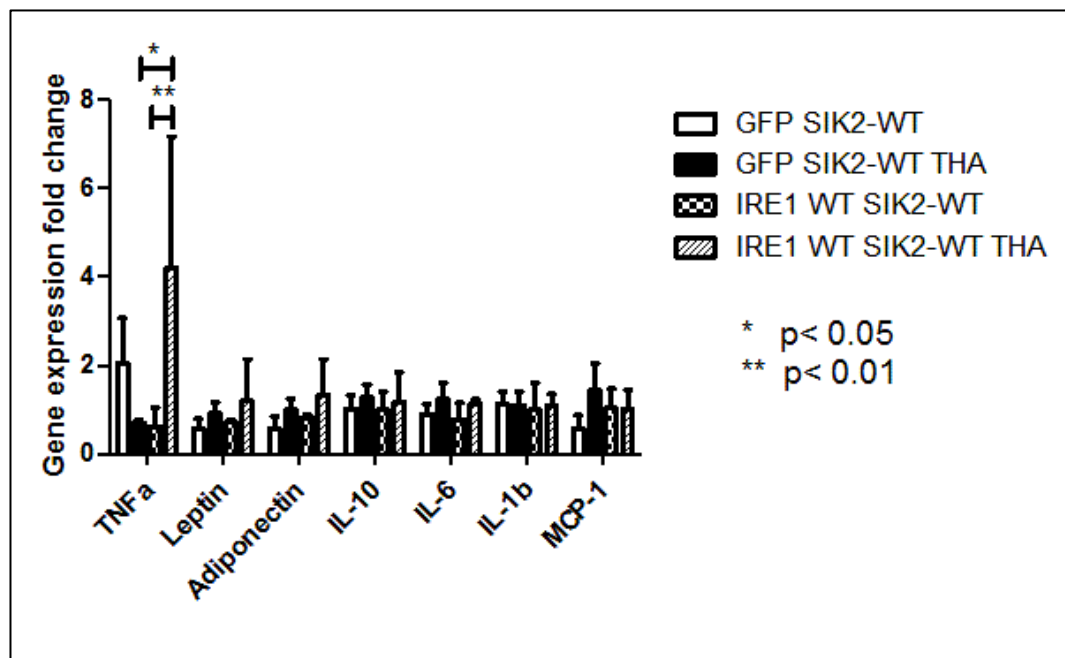


Figure 9.6: Gene expression changes of LiSa-2 GFP and IRE1-WT cells upon SIK2-WT transfection and thapsigargin treatment.

Upon SIK2 overexpression mediated by transient transfection and ER Stress induced by Thapsigargin; Leptin, Adiponectin, IL-10, IL-6 and MCP-1 genes were upregulated in LiSa-2 GFP cells. Only the level of TNF $\alpha$  was downregulated in these cells. In IRE1-WT cells, ER stress caused upregulation of Leptin, Adiponectin, IL-10, IL-6. On the other hand, Tha treatment did not have major effects on gene expression alterations of IL-1 $\beta$  and MCP-1. ER stress has caused a significant change only in TNF $\alpha$  level compared with the other genes. TNF $\alpha$  expression was upregulated approximately 4 folds higher than non-treated thapsigargin group. IRE1 overexpression with thapsigargin treatment showed significant upregulation compared with the control group LiSa-2 GFP cells (Figure 9.6).

## 9.5. Gene Expression Levels of LiSa-2 GFP and IRE1<sup>K888A</sup> Stable Cell Lines

In this experiment, the effects of the RNase domain mutated IRE1<sup>K888A</sup> cell line on the gene expression were observed. Same experimental setup performed with IRE1-WT was used. SIK2-WT and HA plasmids were transiently transfected to the LiSa-2 GFP and IRE1<sup>K888A</sup> cells. After 24 hours, 1  $\mu$ M Thapsigargin was added and it was incubated with 24 hours. Then the cells were collected for RNA isolation. Subsequent cDNA synthesis followed q-pcr analysis. The expression profiles of TNF $\alpha$ , Leptin and IL-6 were analyzed. Upon ER stress induced by Thapsigargin, the expression of all three genes were upregulated in the control SIK2-WT transfected GFP cells. The levels of TNF $\alpha$  and Leptin were downregulated due to the effect of Thapsigargin in IRE1<sup>K888A</sup> cells. However, the IL-6 gene expression was upregulated upon ER stress in IRE1<sup>K888A</sup> cells compared with the control groups. With ER stress, a significant change has been observed between the control GFP and IRE1<sup>K888A</sup> cells (Figure 9.7).

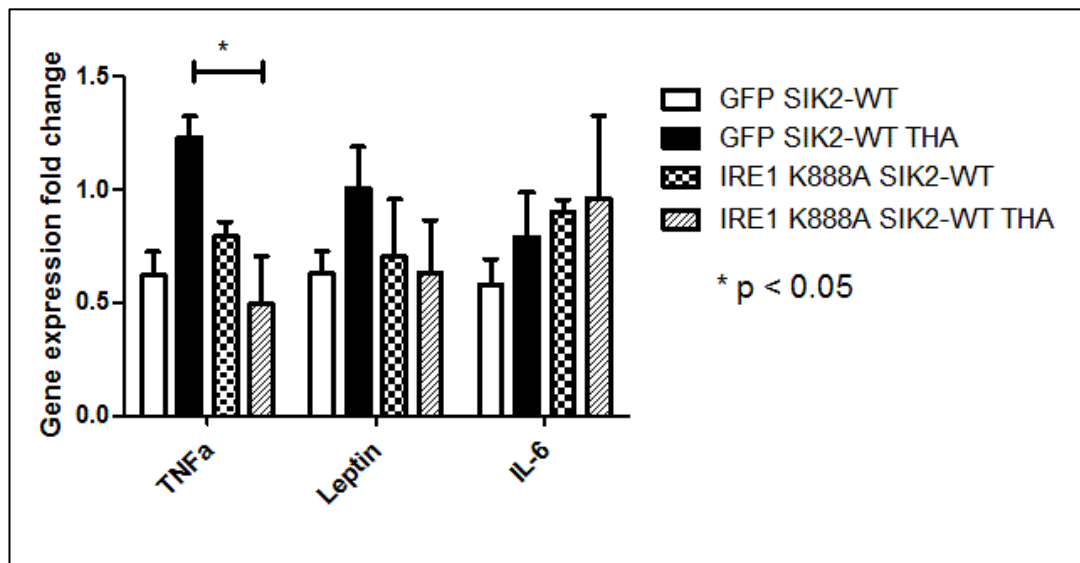


Figure 9.7: Gene expression changes of LiSa-2 GFP and IRE1<sup>K888A</sup> cells upon SIK2-WT transfection and thapsigargin treatment.

## 9.6. Comparison of Gene Expression Levels Between LiSa-2 IRE1-WT and IRE1<sup>K888A</sup> Stable Cell Lines

According to the results obtained from the q-pcr analysis, all the three stable cell lines of LiSa-2 GFP, IRE1-WT and IRE1<sup>K888A</sup> were compared with each other. The TNF $\alpha$  levels have shown significant changes. Thapsigargin treatment has shown a significant upregulation of TNF $\alpha$  level in IRE1-WT cells compared with itself and control GFP cells with or without ER stress. ER stress created IRE1-WT cells have shown a remarkable changes in TNF $\alpha$  levels compared with stressed and non-stressed IRE1<sup>K888A</sup> cells. On the other hand, Thapsigargin did not show prominent alterations in IRE1<sup>K888A</sup> cells in the expression levels of TNF $\alpha$ , Leptin and IL-6 (Figure 9.8).

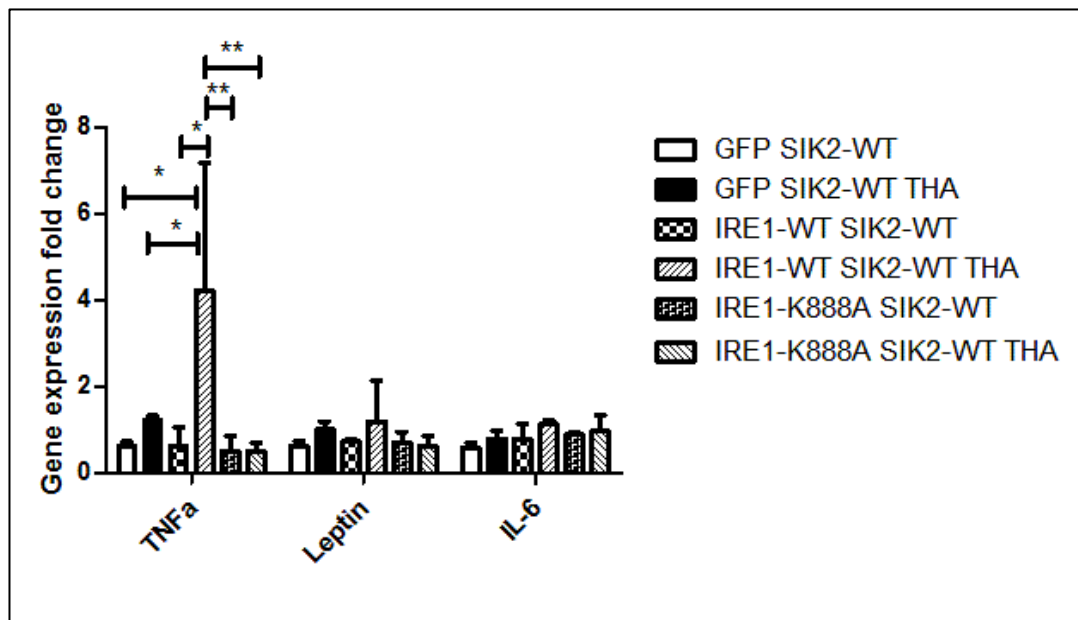


Figure 9.8: Comparison of gene expression levels between LiSa-2 IRE1-WT and IRE1<sup>K888A</sup> cells upon SIK2-WT transfection and thapsigargin treatment.

## 10. DISCUSSION

The rise of obesity epidemic worldwide constitute the major risk factor for the development of various metabolic and age related neurodegenerative diseases like Alzheimer and some cancer types. Although different in nature all these diseases are linked to irreversible deterioration of ER homeostasis presumably due to accumulation of unfolded/misfolded protein aggregates in different location of the affected cells. Therefore, improving protein folding capacity and quality along with the enhanced clearance of protein aggregates from the afflicted cells will open the way for the new therapeutic strategies for these diseases.

SIK2 level and activity has been shown to decrease in white adipose tissue of obese individuals. It is known that in obese animal models and human subjects various metabolic and brain tissues experience chronic ER stress leading to low grade inflammatory state so called metainflammation. The reduced level and activity of SIK2 in adipose tissue of obese human subjects encouraged us to test its role in inflammatory response by looking at the secretory profiles of adipocytes modified to stably express IRE1 $\alpha$  in the presence or absence of SIK2 activity provided transiently under ER stress conditions. IRE1 is the major sensor of UPR and relay signal through its RIDD activity to modulate translation of secretory protein on ER membrane. Taken together with our earlier report that SIK2 activity is capable of altering the adipokine profile in murine adipocytes in response to ER stress we speculated that if these two signaling pathway are somehow interrelated. The conditions that trigger ER stress are the disruption of cellular processes such as protein synthesis, folding and secretion. Upon this disruption, ER homeostasis imbalance activates an adaptive response defined as unfolded protein response (UPR). The aim of UPR is to restore the ER homeostasis by stimulating the stress sensors; IRE-1, PERK, and ATF-6. Each signaling pathway copes with ER stress by diminishing global protein synthesis and increasing folding capacity of ER. Cells also use ER Associated Degradation (ERAD) to get over the overload in ER. If these pathways cannot restore ER homeostasis, the fate of cell is directed to the apoptosis by activation of several apoptotic pathways. Upon the chronic and unrestored ER stress, IRE1 $\alpha$  activates the Regulated IRE1 $\alpha$  Dependent Decay (RIDD). This mechanism determines the cell fate and apoptosis is activated.

Recent studies revealed that SIK2 plays a role in several biological mechanisms such as insulin signaling, adipogenesis, gluconeogenesis and inflammation. It has shown that the inflammations and chronic ER stress in obese individuals cause impairment in the pathways controlling the gluconeogenesis and lipogenesis. The experiments done with SIK2 knockout mice models showed that SIK2 is required for adipocyte differentiation. Moreover, in adipocytes, the activation of PKA, the upstream of SIK2, causes the phosphorylation of SIK2 which results in binding SIK2 to 14-3-3 proteins. SIK2 inhibition and cytosolic translocation prevent the downstream signaling pathways including CRTC2 and class II Histone deacetylases.

Screaton et al. has shown that the tumour-suppressor kinase LKB1 and its substrates which belong AMPK family cause inhibition of CREB-mediated gene expression by phosphorylating CRTCs. Phosphorylation of CRTC2 and class II HDACs results in binding to 14-3-3 proteins and prevention of their entry to nucleus. Thus the gene expression requiring these factors cannot be initiated. Henriksson et al. showed that LKB1 signalling may be effective in rendering the adipocyte precursors in their non-mature state and adipogenesis can be initiated if the LKB1 signalling attenuates. To reveal this, the expression of LKB1 was stably reduced and the LKB1 knockout mouse embryonic fibroblasts revealed more differentiation level and more triglycerides accumulation. In addition, adipogenic transcription factors of CEBP $\alpha$  and proliferator-activated receptor  $\gamma$  (PPAR $\gamma$ ) were induced to trigger differentiation in the absence of LKB1. On the other hand, the 90% reduction in LKB1 activity did not show the expected larger attenuation of specific downstream substrates such as AMPK and SIK2. While AMPK activity was reduced by 40% in the mice expressing 10% LKB1 activity, SIK2 activity was reduced only 25%. This result brings in mind the existence of alternative upstream kinases that function in the activation of these substrates.

Upon ER stress, IRE1 $\alpha$  initiates either splicing or directs to RIDD to cope with this stress. Also SIK2 plays a major role in protein homeostasis which means ERAD mechanism and autophagy. The common aim of these pathways is to relieve the stress by activating related mechanisms.

Recent studies have shown that protein ubiquitination has a significant role in several cell signaling pathways. For RIG-I activation which is the downstream of RIDD, polyubiquitination of Lysine-63 has been demonstrated as an important factor for the signaling steps for downstream and upstream of Mitochondrial antiviral-

signaling protein (MAVS). Activation of MAVS leads to induction of related protein kinases I $\kappa$ B kinase and TANK Binding Kinase 1 (IKK and TBK1) resulting in the activation of Nuclear Factor- $\kappa$ B (NF- $\kappa$ B) and Interferon regulatory factor 3 (IRF3) transcription factors. As a consequence, they initiate the expression of antiviral molecules in the nucleus. The studies have revealed that viral RNAs including 5'-triphosphate and dsRNAs are the specific ligands which can activate RIG-I pathway. The viral RNA binding to the RIG-I causes its dimerization and triggers the ATPase activity. With the energy gained from hydrolysis of ATP, further RIG-I binding can be facilitated. Any mutations affecting the activity of ATPase domain can be carried out to observe the results on the downstream pathways. It has been shown that a mutation localized in ATPase domain has abolished the induction of interferons by RIG-I. The CARD domains of RIG-I serve as protein interaction regions and have an important role in inflammation and apoptosis. Wenwen et al. have discovered the specific binding of these CARD domains to the K63 polyUb chains. To test the RIG-I activation, mutations disrupting the ubiquitin binding of RIG-I can be performed to see the effects on the downstream signaling pathways. Performed mutations displayed impairment in the ability of RIG-I to activate IRF3 proving that binding of polyUb is a major factor for the activation of RIG-I.

Previous studies show that under ER stress conditions, IRE1 has a capability of determining the cell fate, survival or death. Because IRE1 RNase activity is required for both XBP/HAC1 splicing and RIDD substrates cleavage, R1039 residue in yeast IRE1 engage in binding of HAC1 has been mutated. R1039A mutation resulted in the diminished RNase activity for splicing HAC1 RNA but remained active for RIDD cleavage. Structural alignment of reported yeast and human 3D structures unraveled functional equivalent of yeast R1039 in human as K888.

Thapsigargin treatment with SIK2 overexpression has shown an increase in Leptin, Adiponectin, IL-6, IL-10 in IRE1-WT cells. The expressions of IL-1 $\beta$  and MCP-1 did not show remarkable change with ER stress. Except TNF $\alpha$ , Thapsigargin treatment with SIK2 overexpression did not have major effect on gene expression changes in IRE1-WT cells. Pro-inflammatory cytokines (IL-6, Leptin, TNF $\alpha$ ) upregulation with ER stress in IRE1-WT cells could be the sign of the inflammation initiation. SIK2 has shown to suppress anti-inflammatory IL-10 production via phosphorylating CRT3 that results in its cytosolic sequestration by 14-3-3 proteins. It has been considered to inhibit SIK2 for effective increase of IL-10 levels [Clark et

al., 2012]. According to these studies, showing not significant increase in IL-10 expression levels with SIK2 overexpression is consistent with the literature. With ER stress, anti-inflammatory cytokine production is inhibited via SIK2 and inflammatory response is triggered.

Stable cell line establishment of RNase domain mutated IRE1<sup>K888A</sup> in LiSa-2 cells seemed promising according to Western Blot results and it was used for the same experimental setup. Thus, same experiment was repeated with stable IRE1<sup>K888A</sup> cells under Thapsigargin treatment and SIK2 overexpression. It was a concern how this mutation at LYS888 residue related with the RNase activity of IRE1 affect the adipocyte secretion profile under ER stress conditions. Pro-inflammatory TNF $\alpha$ , Leptin and IL-6 have been picked up to be examined for these cells. Contrary to IRE1-WT cells, TNF $\alpha$  level was downregulated in IRE1<sup>K888A</sup> cells with SIK2 overexpression upon Thapsigargin treatment. This shows that the IRE1<sup>K888A</sup> cells could relieve the ER stress by decreasing the protein overload to the ER by means of mRNA cleavage with activating its RIDD mechanism. Comparing with the control ER-stressed GFP cells, IRE1<sup>K888A</sup> cells have shown a significant decrease in TNF $\alpha$  level in spite of presence of ER stress. While Leptin was showing the same profile with TNF $\alpha$ , IL-6 expression was conversely upregulated. Upon mutation in the RNase domain in IRE1, the TNF $\alpha$  level has showed a decrease compared with the results obtained with IRE1-WT cells. With this mutation, it was aimed to block the survival pathway of IRE1 through XBP-1 splicing, instead of it, the cleavage activity of RIDD mechanism was considered to be enhanced with creating ER stress via Thapsigargin treatment. By blocking the XBP-splicing survival pathway, the cells could cope with the ER stress and may prevent the inflammation initiation by correlating the decrease in TNF $\alpha$  levels. This brings in mind that this mutation may be the effective step for further studies to prevent the inflammatory response by overcoming the stress when the cells faced with it.

The TNF $\alpha$  levels in control GFP cells have shown different expression levels in the experiments performed at different times. Passaging of these cells may result in a change of secretion profile. In any case, this experimental setup should be repeated to get more trustworthy results.

The kinetics of RIDD and XBP1 splicing might show difference according to the cell type and the nature of ER stress. As a consequence, overall outcomes may be changed. Further experiments are necessary to lighten this part of the study. Thus, painstaking judgments concerning the functional effects between XBP1 splicing and

RIDD activation will contribute a better understanding of how SIK2 affects the adipocyte secretome under ER stress through IRE1 pathway and also provide the justifications for development of new, effective treatments and drugs for the ER stress relevant diseases.

## REFERENCES

- Ahima R. S., Flier J. S., (2000), "Adipose tissue as an endocrine organ", *Trends Endocrinology Metabolism*, 11, 327–32.
- Ali M. M. U., (2011), "Structure of the Ire1 autophosphorylation complex and implications for the unfolded protein response", *EMBO Journal*, 30, 894–905.
- Anelli T., Sitia R., (2008), "Protein quality control in the early secretory pathway", *EMBO Journal*, 27, 315–327.
- Ashcroft F. M., Rorsman P., (2012), "Diabetes mellitus and the beta cell: the last ten years", *Cell*, 148, 1160–1171.
- Baumann O., Walz B., (2001), "Endoplasmic reticulum of animal cells and its organization into structural and functional domains", *International Review of Cytology*, 205, 149–214.
- Bertolotti A., Zhang Y., Hendershot L. M., Harding H. P., Ron D., (2000), "Dynamic interaction of BiP and ER stress transducers in the unfolded-protein response", *Nature Cell Biology*, 2, 326–332.
- Bukau B., Weissman J., Horwich A., (2006), "Molecular chaperones and protein quality control", *Cell*, 125, 443–45.
- Butler A. E., Janson J., Bonner-Weir S., Ritzel R., Rizza R. A., Butler P. C., (2003), "Beta-cell deficit and increased beta-cell apoptosis in humans with type 2 diabetes", *Diabetes*, 52, 102–110.
- Chandran M., Phillips S. A., Ciaraldi T., Henry R. R., (2003), "Adiponectin: More than just another fat cell hormone?", *Diabetes Care*, 26, 2442–2450.
- Chang L., Chiang S. H., Saltiel A. R., (2004), "Insulin signaling and the regulation of glucose transport", *Molecular Medicine*, 10, 65–71.
- Clark K., MacKenzie K. F., Petkevicius K., Kristariyanto Y., Zhang J., Choi H. G., Cohen P., (2012), "Phosphorylation of CRT3 by the salt-inducible kinases controls the interconversion of classically activated and regulatory macrophages", *Proceedings of the National Academy of Sciences*, 109, 16986–16991.
- Cox J. S., Shamu C. E., Walter P., (1993), "Transcriptional induction of genes encoding endoplasmic reticulum resident proteins requires a transmembrane protein kinase", *Cell*, 73, 1197–1206.
- Darling N. J., Toth R., Arthur J. S. C., Clark K., (2016), "Inhibition of SIK2 and SIK3 during differentiation enhances the anti-inflammatory phenotype of macrophages", *Biochemical Journal*, 474, 4, 521–537.

Dobson C. M., Sali A., Karplus M., (1998), "Protein folding: a perspective from theory and experiment", *Angewandte Chemie International Edition*, 7, 868–893.

Ellgaard L., Helenius A., (2003), "Quality control in the endoplasmic reticulum", *Nature Reviews Molecular Cell Biology*, 4, 181–191.

Ellgaard L., Molinari M., Helenius A., (1999), "Setting the standards: quality control in the secretory pathway", *Science*, 286, 1882–1888.

Fernandez-Real J. M., Ricart W., (2003), "Insulin resistance and chronic cardiovascular inflammatory syndrome", *Endocrinology Reviews*, 24, 278–301.

Fewell S. W., Travers K. J., Weissman J. S., Brodsky J. L., (2001), "The action of molecular chaperones in the early secretory pathway", *Annual Review of Genetics*, 35, 149–191.

Flier J. S., (2004), "Obesity wars: molecular progress confronts an expanding epidemic", *Cell*, 116, 337–350.

Fonseca-Alaniz M. H., Takada J, Alonso-Vale M. I. C., Lima F. B., (2007), "Adipose tissue as an endocrine organ: from theory to practice", *Journal of Pediatrics*, 83,192–203.

Gordon E. S., (1964), "Lipid metabolism, diabetes mellitus and obesity" *Journal of Advances in Internal Medicine*, 12, 66–102.

Gorlach A, Klappa P, Kietzmann T., (2006), "The endoplasmic reticulum: folding, calcium homeostasis, signaling, and redox control", *Antioxid Redox Signal*, 8, 1391–1418.

Gual P., Marchand-Brustel Y. L., Tanti J. F., (2005), "Positive and Negative Regulation of Insulin Signaling Through IRS-1 Phosphorylation", *Biochimie*, 87, 99–109.

Hampton R. Y., (2002), "ER-associated degradation in protein quality control and cellular regulation", *Current Opinion in Cell Biology*, 14, 476–482.

Han, D., (2009), "IRE1 alpha kinase activation modes control alternate endoribonuclease outputs to determine divergent cell fates", *Cell*, 138, 562–575.

Harding H. P., Zhang Y., Ron D., (1999), "Protein translation and folding are coupled by an endoplasmic-reticulum-resident kinase", *Nature*, 397, 271–274.

Haze K., Yoshida H., Yanagi H., Yura T., Mori K., (1999), "Mammalian Transcription Factor ATF6 Is Synthesized as a Transmembrane Protein and Activated by Proteolysis in Response to Endoplasmic Reticulum Stress", *Molecular Biology of the Cell*, 10 (11), 3787–3799.

Helenius A., Aebiz M., (2004), "Roles of N-Linked Glycans in the Endoplasmic Reticulum", *Annual Review of Biochemistry*, 73, 1019–1049.

Hetz C., Glimcher L. H., (2009), “Fine-tuning of the unfolded protein response: assembling the IRE1 alpha interactome”, *Molecular Cell*, 35, 551–561.

Hetz C., Martinon F., Rodriguez D., Glimcher L. H., (2011), “The unfolded protein response: integrating stress signals through the stress sensor IRE1 $\alpha$ ”, *Physiological Reviews*, 91, 1219–1243.

Hollien J., (2009), “Regulated Ire1-dependent decay of messenger RNAs in mammalian cells”, *Journal of Cell Biology*, 186, 323–331.

Hoppe T., Matuschewski K., Rape M., Schlenker S., Ulrich H. D., Jentsch, S., (2000), “Activation of a membrane-bound transcription factor by regulated ubiquitin/proteasome-dependent processing”, *Cell*, 102, 577–586.

Horike N., Takemori H., Katoh Y., Doi J., Min L., Asano T., Sun X. J., Yamamoto H., Kasayama S., Muraoka M., Nonaka Y., Okamoto M., (2003), “Adipose-Specific Expression, Phosphorylation of Ser794 in Insulin Receptor Substrate-1 and Activation in Diabetic Animals of Salt-Inducible Kinase-2”, *Journal of Biological Chemistry*, 278, 18440-18447.

Hubbard S. C., Ivatt R. J., (1981), “Synthesis and processing of asparagine-linked oligosaccharides”, *Annual Review of Biochemistry*, 50, 555–583.

Ibrahim M. M., (2010), “Subcutaneous and visceral adipose tissue: structural and functional differences”, *Obesity Reviews*, 11, 11–18.

Janssens S., Pulendran B., Lambrecht B. N., (2014), “Emerging functions of the unfolded protein response in immunity”, *Nature Immunology*, 15,10, 910-919.

Katoh Y., Takemori H., Doi J., Okamoto M., (2002), “Identification of the nuclear localization domain of salt-inducible kinase”, *Endocrine Research*, 28, 315- 318.

Katoh Y., Takemori H., Horike N., Doi J., Muraoka M., Min L., Okamoto M., (2004), “Salt-inducible kinase (SIK) isoforms: their involvement in steroidogenesis and adipogenesis”, *Molecular and Cellular Endocrinology*, 217, 109-112.

Kaufman R. J., (1999), “Stress signaling from the lumen of the endoplasmic reticulum: coordination of gene transcriptional and translational controls”, *Genes & Development*, 13,1211–1233.

Korennykh A. V., Pascal F. E., Korostelev A. A., Zhang C., Shokat K. M., Stroud R. M., Walter P., (2009), “The unfolded protein response signals through high-order assembly of Ire1” *Nature*, 457, 687–693.

Korennykh A. V., Korostelev A. A., Egea P. F., Finer-Moore J., Stroud R. M., Zhang C., Shokat K. M., Walter P., (2011), “Structural and functional basis for RNA cleavage by Ire1”, *BioMed Central Biology*, 9, 47.

Kreibich G., Ulrich, B. L., Sabatini, D. D., (1978), “Proteins of rough microsomal membranes related to ribosome binding: 1. Identification of ribophorins I and II,

membrane proteins characteristic of rough microsomes”, *The Journal of Cell Biology*, 77, 464–487.

Kwon H., Pessin J. E., (2013), “Adipokines mediate inflammation and insulin resistance”, *Frontiers in Endocrinology*, 4,71.

Lee K. P., De M., Neculai D., Cao C., Dever T. E., Sicheri F., (2008b), “Structure of the dual enzyme Ire1 reveals the basis for catalysis and regulation in nonconventional RNA splicing”, *Cell*, 132, 89-100.

Lencer W. I., DeLuca H., Grey M. J., Cho J. A., (2015), “Innate Immunity at Mucosal Surfaces: the IRE1-RIDD-RIG-I Pathway”, *Trends in Immunology*, 36,7, 401–409.

Lin J. H., (2007), “IRE1 signaling affects cell fate during the unfolded protein response”, *Science*, 318, 944–949.

Lin J. H., (2009), “Divergent effects of PERK and IRE1 signaling on cell viability”, *PLoS ONE*, 4, e4170.

Lizcano J. M., Göransson O., Toth R., Deak M., Morrice N. A., Boudeau J., Alessi D. R., (2004), “LKB1 is a master kinase that activates 13 kinases of the AMPK subfamily, including MARK/PAR-1”, *The EMBO Journal*, 23, 833–843.

Ma Y., Brewer J.W., Diehl J.A., Hendershot L.M., (2002), “Two distinct stress signaling pathways converge upon the CHOP promoter during the mammalian unfolded protein response”, *The Journal of Molecular Biology*, 318, 1351–1365.

Maffei M., Fei H., Lee G. H., Dani C., Leroy P., Zhang Y., (1995), “Increased expression in adipocytes of ob RNA in mice with lesions of the hypothalamus and with mutations at the db locus”, *Proceedings of the National Academy of Sciences*, 92, 6957-60.

Manning G., Whyte D. B., Martinez R., Hunter T., Sudarsanam S., (2002), “The protein kinase complement of the human genome“, *Science*, 298, 1912–1934.

McCracken A. A., Brodsky J. L., (1996), “Assembly of ER-associated protein degradation in vitro: dependence on cytosol, calnexin, and ATP”, *The Journal of Cell Biology*, 132, 291–298.

Mori K., Ma W., Gething M.J., Sambrook J., (1993), “A transmembrane protein with a cdc2+/CDC28-related kinase activity is required for signaling from the ER to the nucleus”, *Cell*, 74, 743–756.

Novoa I., Zhang Y., Zeng H., Jungreis R., Harding H. P., Ron D., (2003), “Stress-induced gene expression requires programmed recovery from translational repression”, *EMBO Journal*, 22, 1180–7.

Olefsky J. M., Glass C. K., (2010), “Macrophages, inflammation, and insulin resistance”, *Annual Review of Physiology*, 72, 219-246.

Palade G., (1975), "Intracellular aspects of the process of protein synthesis", *Science*, 189, 347–358.

Palade G.E., (1956), "The Endoplasmic Reticulum", *The Journal of Biophysical and Biochemical Cytology*, 2,4, 85-98.

Pannacciulli N., Vettor R., Milan G., Grazotto M., Catucci A., Federspil G., (2003), "Anorexia nervosa is characterized by increased adiponectin plasma levels and reduced nonoxidative glucose metabolism", *The Journal of Clinical Endocrinology and Metabolism*, 88,1748-52.

Papa F. R., Zhang C., Shokat K., Walter P., (2003), "Bypassing a kinase activity with an ATP-competitive drug", *Science*, 302, 1533-1537.

Patel S., Latterich M., (1998), "The AAA team: related ATPases with diverse functions", *Trends in Cell Biology*, 8, 65–71.

Petersen E. W., Carey A. L., Sacchetti M., Steinberg G. R., Macaulay S. L., Febbraio M. A., Pedersen B. K., (2005), "Acute IL-6 treatment increases fatty acid turnover in elderly humans in vivo and in tissue culture in vitro", *American Journal of Physiology - Endocrinology & Metabolism*, 288, 155-62.

Petersen K. F., Shulman G. I., (2006), "Etiology of insulin resistance", *The American Journal of Medicine*, 119,10–16.

Pinhas-Hamiel O, Dolan L. M., Daniels S. R., (1996), "Increased incidence of non-insulin-dependent diabetes mellitus among adolescents", *Journal of Pediatrics*, 128, 608–615.

Rajala M. W., Obici S., Scherer P. E., Rossetti L., (2003), "Adipose-derived resistin and gut-derived resistin-like molecule- selectively impair insulin action on glucose production", *Journal of Clinical Investigation*, 111, 225–230.

Ron D., Walter P., (2007), "Signal integration in the endoplasmic reticulum unfolded protein response", *Nature Reviews Molecular Cell Biology*, 8, 519–529.

Saely C., Geiger K., Drexel H., (2012), "Browns versus white adipose tissue: a mini review", *The Journals of Gerontology*, 58, 120–2.

Schafer K., Fujisawa K., Konstantinides S., Loskutoff D. J., (2001), "Disruption of the plasminogen activator inhibitor 1 gene reduces the adiposity and improves the metabolic profile of genetically obese and diabetic ob/ob mice" , *FASEB Journal*, 15:1840–1842.

Scheuner D., Song B., McEwen E., Gillespie P., Saunders T., Bonner-Weir S., Kaufman R. J., (2001), "Translational control is required for the unfolded protein response and in-vivo glucose homeostasis", *Molecular Cell*, 7, 1165-1176.

Schroder M., (2008), "Endoplasmic reticulum stress responses", *Cellular and Molecular Life Sciences*, 65: 862–894.

Schroder M., Kaufman R. J., (2005), "The mammalian unfolded protein response", *Annual Review of Biochemistry*, 74, 739–789.

Screaton R. A., Conkright M. D., Katoh Y., Best J. L., Canettieri G., Jeffries S., Guzman E., Niessen S., Yates J. R., Takemori H., (2004), "The CREB coactivator TORC2 functions as a calcium- and cAMP-sensitive coincidence detector", *Cell*, 119, 61–74.

Seiser R. M., (2000), "The Fate of Membrane-bound Ribosomes Following the Termination of Protein Synthesis", *The Journal of Biological Chemistry*, 275, 33820-33827.

Shen J., Prywes R., (2004), "Dependence of site-2 protease cleavage of ATF6 on prior site-1 protease digestion is determined by the size of the luminal domain of ATF6", *The Journal of Biological Chemistry*, 279, 43046–43051.

Sidrauski C., Walter P., (1997), "The transmembrane kinase Ire1p is a site-specific endonuclease that initiates mRNA splicing in the unfolded protein response", *Cell*, 90, 1031-1039.

Sonksen P., Sonksen J., (2000), "Insulin: understanding its action in health and disease", *British Journal of Anaesthesia*, 85, 69-79.

Steinberger J., Moorehead C., Katch V., (1995), "Relationship between insulin resistance and abnormal lipid profile in obese adolescents", *Journal of Pediatrics*, 126, 690–695.

Stith R. D., Luo J., (1994), "Endocrine and carbohydrate responses to interleukin-6 in vivo", *Circulatory Shock*, 44, 210–215.

Tajiri Y., Mimura K., Umeda F., (2005), "High-sensitivity C-reactive protein in Japanese patients with type 2 diabetes", *Obesity research*, 13(10), 1810-1816.

Tam A. B., Koong A. C., Niwa M., (2014), "Ire1 Has Distinct Catalytic Mechanisms for XBP1/HAC1 Splicing and RIDD", *Cell Reports*, 9(3), 850–858.

Upton J. P., (2012), "IRE1alpha cleaves select microRNAs during ER stress to derepress translation of proapoptotic caspase-2", *Science*, 338, 818–822.

Urbina E. M., Gidding S. S., Bao W., (1999), "Association of fasting blood sugar level, insulin level, and obesity with left ventricular mass in healthy", *American Heart Journal*, 138, 122-7.

Uysal K. T., Wiesbrock S. M., Marino M. W., Hotamisligil G. S., (1997), "Protection from obesity-induced insulin resistance in mice lacking TNF- $\alpha$  function", *Nature*, 389, 610–614.

Vembar S. S., Brodsky J. L., (2008), "One step at a time: Endoplasmic Reticulum-Associated Degradation", *Nature Reviews Molecular Cell Biology*, 9, 944-957.

Vidal-Puig A., O’Rahilly S., (2001), “Resistin: A new link between obesity and insulin resistance?”, *Clinical Endocrinology*, 55, 437–438.

Vozarova B., Weyer C., Hanson K., Tataranni P. A., Bogardus C., Pratley R.E., (2001), “Circulating interleukin-6 in relation to adiposity, insulin action and insulin secretion”, *Obesity Research*, 9, 414–417.

Walter P., Ron D., (2001), “The unfolded protein response: from stress pathway to homeostatic regulation”, *Science*, 334, 1081–1086.

Wang M., Kaufman R. J., (2014), “The impact of the endoplasmic reticulum protein-folding environment on cancer development”, *Nature Reviews Cancer*, 14,9, 581–597.

Wang Q., Song C., Li C. C., (2004), “Molecular perspectives on p97-VCP: progress in understanding its structure and diverse biological functions”, *Journal of Structural Biology*, 146, 44–57.

Weisberg S. P., McCann D., Desai M., Rosenbaum M., Leibel R. L., Ferrante A. W. Jr., (2003), “Obesity is associated with macrophage accumulation in adipose tissue”, *The Journal of Clinical Investigation*, 112, 1796–1808.

Yamamoto K., Yoshida H., Kokame K., Kaufman R. J., Mori K., (2004), “Differential contributions of ATF6 and XBP1 to the activation of endoplasmic reticulum stress-responsive cis-acting elements ERSE, UPRE and ERSE-II”, *The Journal of Biochemistry*, 136, 343–350.

Yang F. C., Lin Y. H., Chen W. H., (2013) “Interaction between Salt-inducible Kinase 2 (SIK2) and p97/Valosin-containing Protein (VCP) Regulates Endoplasmic Reticulum (ER)-associated Protein Degradation in Mammalian Cells”, *The Journal of Biological Chemistry*, 228 (47), 33861- 33872.

Ye Y., Meyer H. H., Rapoport T. A., (2003), “Function of the p97-Ufd1-Npl4 complex in retrotranslocation from the ER to the cytosol: dual recognition of nonubiquitinated polypeptide segments and polyubiquitin chains”, *Journal of Cell Biology*, 162, 71–84.

Ye Y., Shibata Y., Yun C., Ron D., Rapoport T. A., (2004), “A membrane protein complex mediates retro-translocation from the ER lumen into the cytosol”, *Nature*, 429, 841–847.

Yoshida H., Matsui T., Yamamoto A., Okada T., Mori K., (2001), “XBP1 mRNA is induced by ATF6 and spliced by IRE1 in response to ER stress to produce a highly active transcription factor”, *Cell*, 107, 881–891.

Zeng W., Sun L., Jiang X., Chen X., Hou F., Adhikari A., Chen Z. J., (2010), “Reconstitution of the RIG-I Pathway Reveals a Pivotal Role of Unanchored Polyubiquitin Chains in Innate Immunity”, *Cell*, 141, 2, 315–330.

Zhang K., Kaufman R.J., (2004), “Signaling the unfolded protein response from the endoplasmic reticulum”, *Journal of Biological Chemistry*, 279, 25, 25935–8.

Zhang L., Zhang C., Wang A., (2016), “Divergence and Conservation of the Major UPR Branch IRE1-bZIP Signaling Pathway across Eukaryotes”, *Scientific Reports*, 6, 27362.

## **BIOGRAPHY**

Nazlı Ertürk was born in Erzincan, Turkey, in 1990. She graduated from Alp Oğuz Anatolian High School. She earned her bachelor's degree in Genetics and Bioengineering from Yeditepe University, Istanbul, Turkey, in 2013. She joined Gebze Technical University, Graduate School of Natural and Applied Sciences, Department of Molecular Biology and Genetics, in February 2014 and graduated in February 2017.

# APPENDICES

## Appendix A: Primer List

Table A1.1: Primers used for quantitative Real-Time PCR Experiments.

Gene Name	Forward Primer (5' to 3') / T <sub>m</sub>	Reverse Primer (5' to 3') / T <sub>m</sub>
<b>RPLP0</b>	AGCCCAGAACACTGGTCTC /60.9	ACTCAGGATTTCAATGGTGCC /60.3
<b>TNF<math>\alpha</math></b>	CCTCTCTAATCAGCCCTCTG /60.8	GAGGACCTGGGAGTAGATGAG /60.2
<b>Leptin</b>	TGCCTTCCAGAAACGTGATCC /62.4	CTCTGTGGAGTAGCCTGAAGC /61.9
<b>Adiponectin</b>	AACATGCCCATTCGCTTTACC /61.3	TAGGCAAAGTAGTACAGCCCA /60.2
<b>IL-6</b>	ACTCACCTCTTCAGAACGAATTG /60.2	CCATCTTGGAAGGTTTCAGGTTG /61.3
<b>IL-1<math>\beta</math></b>	ATGATGGCTTATTACAGTGGCAA /60.0	GTCGGAGATTCGTAGCTGGA /60.8
<b>IL-10</b>	GACTTTAAGGGTTACCTGGGTTG /60.5	TCACATGCGCCTTGATGTCTG /63.0
<b>MCP-1</b>	CAGCCAGATGCAATCAATGCC /62.3	TGGAATCCTGAACCCACTTC /60.4